2015-06-12

Recent investigations of the 0-5 geomagnetic field recorded by lava flows

Johnson, Catherine L.

Recent Investigations of the 0-5 Ma Geomagnetic Field Recorded by Lava Flows

Catherine L. Johnson[1,2], **Catherine G. Constable**[2], **Lisa Tauxe**[2]
René Barendregt[3], **Laurie L. Brown**[4], **Rob Coe**[5], **Phil Gans**[6]
Paul Layer[7], **Vicky Mejia**[8], **Neil D. Opdyke**[9]
Brad Singer[10], **Hubert Staudigel**[2], **David Stone**[7]

Corresponding author: Catherine L. Johnson
[1]Department of Earth and Ocean Sciences, University of British Columbia
6339 Stores Road, Vancouver, B.C. V6T 1Z4. Canada.
email: cjohnson@eos.ubc.ca

[2]Scripps Institution of Oceanography, University of California San Diego, La Jolla, CA 92093
[3] University of Lethbridge, Alberta, Canada
[4] University of Massachussetts
[5] University of California, Santa Cruz
[6] University of California, Santa Barbara
[7] University of Alaska
[8] Vicky - new affiliation???
[9] University of Florida
[10] University of Wisconsin

Draft October 13, 2006

Abstract

We present a synthesis of paleomagnetic directional data collected from 873 lava flows at 17 different locations under the collaborative Time Averaged geomagnetic Field Initiative (TAFI). The data range from 0-5 Ma in age, and provide new high quality data with improved spatial coverage. Data quality at each site is measured using k, the best estimate of the Fisherian precision parameter, and its influence on inclination anomaly and VGP dispersion is evaluated by systematically excluding data with successively higher values of k. When combined with regional compilations from NW USA, SW USA, Japan, New Zealand, Hawaii, Mexico, S. Pacific and the Indian Ocean, a data set of 2283 pairs of declination and inclination data, with k>100, and VGP latitudes greater than 45° is obtained. This is a more than 7-fold increase over similar quality data in the existing Global Paleomagnetic Database (GPMDB). The new data set spans 78°S to 53°N, and has sufficient temporal and spatial sampling to allow characterization of latitudinal variations in the time-averaged field (TAF) and paleosecular variation (PSV) for the Brunhes and Matuyama epochs, and for the 0–5 Myr interval combined. PSV, as measured by dispersion of virtual geomagnetic poles, shows less latitudinal variation than predicted by current statistical PSV models. Variation of inclination anomaly with latitude is assessed using 2-parameter zonal TAF models – these have axial quadrupole contributions of 2% – 4% of the axial dipole term, and axial octupole contributions of 3% – 5%. Approximately 2% of the octupole signature is likely the result of bias incurred by averaging unit vectors. The new data set provides significant improvement over previous compilations, and can contribute to a new generation of global paleomagnetic field models.

1. Introduction

The structure and evolution of the magnetic field is key to understanding the geodynamo and Earth's deep interior, but many aspects of it remain poorly documented particularly on time scales of 10^4 to 10^6 years. While paleomagnetists have made extensive use of the approximation of the time-averaged geomagnetic field by a geocentric axial dipole (GAD), it has been known for some time [*Wilson & Ade-Hall*, 1970], that there are systematic departures from this simple model. The nature of departures from GAD over the past few million years is debated [*Gubbins & Kelly*, 1993; *Kelly & Gubbins*, 1997; *Johnson & Constable*, 1995, 1997; *Merrill et al.*, 1996; *McElhinny et al.*, 1996; *Carlut and Courtillot*, 1998], and controversy over field structure extends to time scales of 10^8 years and longer [*Piper & Grant*, 1989; *Kent & Smethurst*, 1998; *Van der Voo & Torsvik*, 2001; *Torsvik & Van der Voo*, 2002; *McFadden*, 2004], for which data sets are even sparser in their geographic and temporal sampling. Experiments with the size and nature of the inner core, and with thermal boundary conditions in numerical dynamo simulations [*Hollerbach & Jones*, 1993a,b; *Glatzmaier et al.*, 1999; *Kono & Roberts*, 2002; *Christensen & Olson*, 2003], suggest that non-GAD field structure may persist over time scales governed by the persistence of the boundary conditions and demonstrate the need to quantify such structure based on measurements of Earth's magnetic field.

Models of the geomagnetic field can be constructed using a spherical harmonic representation. The magnetic scalar potential in a source free region due to an internal field obeys Laplace's equation, and can be written as

$$\Psi(r,\theta,\phi,t) = a\sum_{l=1}^{\infty}\sum_{m=0}^{l}\left(\frac{a}{r}\right)^{l+1}\left(g_l^m(t)\cos m\phi + h_l^m(t)\sin m\phi\right)\ P_l^m(\cos\theta) \tag{1}$$

where $g_l^m(t)$ and $h_l^m(t)$ are the Schmidt partially normalized Gauss coefficients at a time t, a is the radius of the Earth, r, θ and ϕ are radius, colatitude and longitude respectively, and P_l^m are the partially normalized Schmidt functions. The magnetic field, $\vec{B}$, is the gradient of the potential Ψ, and a field model is specified by the Gauss coefficients $g_l^m(t)$ and $h_l^m(t)$. The $m = 0$ terms correspond to spherical harmonic functions with no azimuthal structure - *i.e.*, they are axially symmetric or zonal. g_1^0, g_2^0, and g_3^0 are the Gauss coefficients representing the axial dipole, axial quadrupole and axial octupole terms, respectively. Time-varying field models can be constructed from time series of magnetic field observations using a parametrization in time (typically cubic b-splines). Regularization of models in both time and space minimizes structure that is not required by the data [*Parker*, 1994]. Observatory and satellite measurements provide $\left(B_x, B_y, B_z\right)$, the north, east, and downward pointing, locally orthogonal magnetic field components. Paleomagnetic observations are typically measurements of direction – declination (D) and inclination (I) – and /or intensity $|B|$, where

$$D = \tan^{-1}\left(\frac{B_y}{B_x}\right), \qquad I = \tan^{-1}\left(\frac{B_z}{\left(B_x^2 + B_y^2\right)^{\frac{1}{2}}}\right), \qquad |B| = \left(B_x^2 + B_y^2 + B_z^2\right)^{1/2} \tag{2}.$$

Over the historical period, 1590–1990 AD, satellite, observatory, and survey measurements of the geomagnetic field have permitted the construction of a spatially detailed, temporally varying magnetic field model, GUFM1 [*Jackson et al.*, 2000; and see also *e.g.*, *Bloxham et al.*, 1989; *Bloxham & Jackson*, 1992]. Similar types of models have also been produced over millenial time scales from compilations of archeomagnetic directional and paleointensity data, and paleomagnetic directional data from high accumulation-rate sediments. The most recent of these, CALS7K.2, extends from 5000 BC – 1950 AD [*Korte & Constable*, 2005]. Time-varying models, such as GUFM1 and CALS7K.2, can be used to examine the evolution of the geomagnetic field. Our interest here is the time-averaged structure: a representation of this is obtained by averaging each of the models over their respective time intervals. The radial component of the magnetic field, B_r, is shown in Figures 1 (a) and (b) for GUFM1 and CALS7K.2, after downward continuation of the scalar potential to the surface of Earth's core under the assumption that the mantle is an insulator. GUFM1 shows significant non-GAD structure, which has been extensively discussed elsewhere [*Jackson et al.*, 2000], and is generally considered to be strongly influenced by the presence of the inner core and

the associated tangent cylinder. Regions of increased radial flux at high latitudes, commonly referred to as flux lobes, have persisted in much the same locations for 400 years. Low radial field over the north pole has been interpreted as a manifestation of magnetic thermal winds and polar vortices within the tangent cylinder [*Hulot et al.*, 2002; *Olson & Arnou*, 1999; *Sreenivasan & Jones*, 2005; 2006]. Equatorial flux patches that are pronounced in the time-varying version of GUFM1 and in modern satellite models [*e.g.*, *Hulot et al.*, 2002], and that appear to propagate westward in the Atlantic hemisphere, are attenuated in the 400 year temporal average (Figure 1a). When averaged over 0–7 ka, CALS7K.2 (Figure 1b) shows longitudinal structure that suggests the presence of flux lobes seen in the historical field. The radial magnetic field is attenuated in CALS7K.2 compared with GUFM1: the resolution and accuracy is clearly inferior, but averaging of millennial scale secular variation also plays a major role in subduing the structure.

The time interval 0–5 Ma is our primary interest. Three quite different, but representative, field models for this interval are seen in panels (c), (d), and (e) of Figure 1. The simplest one, (c), is based on the premise that only zonal structure can be resolved, and shows B_r at the core-mantle boundary due to an axial dipole, with a zonal quadrupole contribution, g_2^0, of $0.05 g_1^0$. Figures (d) and (e) are constructed using the same techniques of regularized inversion used for GUFM1 and CALS7K.2. These paleofield models are not continuously varying in time, due to the intermittent record provided by volcanic rocks and the poor spatial data distribution. Instead, time-averaged field directions are inverted for a time-averaged field model. In Figures 1(c)-(e), the structure in each model depends on the data sets used: the greatest number of paleodata come from sediment piston cores [*Schneider and Kent*, 1990] with only inclination data and large uncertainties. These are compatible with very smooth models like that shown in (c). When lava flow observations are combined with sediment data, they suggest the muted non-zonal structure in (d) [*Johnson & Constable*, 1997], and lava flow data alone indicate more complex average field structure (Figure 1e) [*Johnson & Constable*, 1995].

Figure 2 shows the signal expected at Earth's surface for the GUFM1, CALS7K.2 and LSN1 average field models, in the form of geographic variations in departures of inclination and declination from GAD predictions. These are given by the inclination anomaly (ΔI) and declination anomaly (ΔD), where

$$\Delta I = I - I_{GAD} \qquad\qquad \Delta D = D \tag{3}$$

The structure in the archeo and paleofield anomalies is rather similar (despite the very different data distributions from which they are derived) and contrasts with that seen in GUFM1. Note that the magnitude of the signal decreases over longer time scales. From Figure 2(f) we see that the average inclination anomaly in LSN1 is rather small, and we can expect the largest signal at equatorial latitudes. If this view of the time-averaged field is approximately correct, then at mid to high latitudes it will be difficult to detect departures from GAD without large data sets that provide accurate measures of ΔI.

Figures 1 and 2 provide the motivation for gathering the new lava flow data presented here, and for assembling large regional data sets from the published literature. Tantalizing similarities among the models averaged on quite different time scales suggest persistent structure in the time-averaged field in the form of high latitude flux lobes, and possible low radial field in polar regions. Such structures are not implausible on several grounds. The inner core tangent cylinder might influence core flow in such a way as to produce persistently high values for B_r in the latitude band occupied by the current flux lobes, and lower values close to the pole. It is also possible that these lobes might exhibit longitudinal bias in their locations as a result of geographically complex variations in thermal conditions at the core-mantle boundary. However, the major limitations in understanding geomagnetic field behavior over relevant time scales (10^6 years and longer) are the quality, temporal distribution and spatial coverage of existing paleomagnetic data.

We examine the role of paleomagnetic directions from volcanics in characterizing the 0–5 Ma time-averaged field (TAF) and its temporal variability or paleosecular variation (PSV). We focus on these data for several reasons. First, volcanics provide geologically instantaneous recordings of field behavior, without the temporal averaging inherent in sedimentary records. Second, measurements of absolute declination provide important constraints on longitudinal structure in the field (see discussion in *Johnson & Constable*, 1997),

and these are often unavailable from deep sea sediment cores. Third, over the past decade data collection efforts by several groups have resulted in many new high quality paleodirections, that can collectively be compared with those used to generate the models shown in Figures 1 and 2.

In PSV studies of lava flows, an estimate of the paleofield at a given location and time is known as a site. At a given site, multiple samples are collected to reduce the influence of measurement error, and these samples must be demagnetized in the laboratory to remove secondary remanence. Site mean values of D and I have an associated uncertainty that reflects within-site scatter. This is usually quoted as the 95% confidence cone about the mean direction, α_{95}, where $\alpha_{95} \approx 140^\circ/\sqrt{kN_s}$ (for k greater than 25) and N_s, k are the number of samples and the estimate of the Fisherian precision parameter, κ respectively. Within-site scatter is sometimes described by the within-site dispersion, s_w, where $s_w = 81^\circ/\sqrt{k}$. Multiple temporally-independent sites are needed to characterize both the TAF and PSV at a single place. A statistic traditionally used to describe PSV is S_B, the root mean square (rms) angular deviation of virtual geomagnetic poles (VGPs) about the geographic axis,

$$S_B = \sqrt{\frac{1}{N-1}\sum_{i=1}^{N}\left(\Delta_i^2 - \frac{S_{w_i}^2}{N_{s_i}}\right)}. \quad (4)$$

Δ_i represents the angular deviation of the pole for the ith site from the geographic north pole, N is the number of sites, and S_B represents the geomagnetic signal remaining after correcting for the within-site dispersion S_{w_i} determined from N_{s_i} samples. (Note that this equation corrects an error in equation (4) of *Lawrence et al.*, 2006). The estimate k for directions can be converted to an approximation to the precision parameter for VGPs using the transformation provided by *Creer* [1962]. The statistical approach inherent in using S_B circumvents the lack of detailed age control and time series of observations that are inevitable in working with lava flows from disparate locations.

While there have been previous attempts to compile global data sets suitable for TAF and PSV modeling [*McElhinny & Merrill*, 1975; *Lee*, 1983; *Quidelleur et al.*, 1994; *Johnson & Constable*, 1996], many issues have persisted, notably those of inadequate (or even unknown) temporal sampling, poor geographical coverage, and poor data quality resulting from inferior laboratory methods. These limitations are the cause of much of the discussion surrounding the level of complexity in the 0–5 Ma TAF. The most conservative view is afforded by *McElhinny & McFadden* [1997; hereafter *MM97*], who in an assessment of a global paleomagnetic database concluded that only 394 D, I pairs would meet modern standards for paleomagnetic research. These data (designated by a demagnetization code '*DMAG 4*' in *MM97*) are restricted to 8 globally distributed locations, and in general have poor age control (Table 1). This does not necessarily mean that the older data are unusable, but has provided a strong incentive to understand the influence of data quality in their interpretation [*e.g.*, *Tauxe et al.*, 2003; *Lawrence et al.*, 2006].

In this paper we provide a synthesis of ongoing work toward new global data compilations for TAF and PSV modeling. In particular, we report the collective results of a major multi-institutional effort - the Time-Averaged Field Investigations (TAFI) project – to improve the characterization of the time-averaged geomagnetic field and paleosecular variation over the past 5 million years. We summarize the numbers of data collected, common field and laboratory procedures, and the resulting temporal and spatial data distribution. We investigate the influence of data quality on estimates of the TAF and PSV from the TAFI data. We supplement the TAFI data with recent published regional compilations, and two new compilations for New Zealand and Japan that we report here. The resulting data set, while not comprehensive, provides a significant improvement over existing global data sets, and we use it to investigate zonal (latitudinal) structure in the TAF and PSV.

2. The Time-Averaged Field Investigations (TAFI) project

Paleomagnetic directions have been obtained from 883 lava flows at 17 locations (Figure 3); we refer to each location as a study. The TAFI study locations were chosen to improve the geographical coverage of

0–5 Ma paleomagnetic directions at high latitudes (Spitzbergen, Aleutians, Antarctica), and in the southern hemisphere (various South American locales, Easter Island and Australia). Several of the TAFI studies were conducted to replace previous, inadequately demagnetized data. Samples in four studies – Aleutians [*Stone and Layer*, 2006; *Coe et al.*, 2000], Antarctica [*Tauxe et al.*, 2004a], Easter Island [*Brown*, 2000] – were collected in the 1960s and 1970s, all other sites required new field work.

New radiometric dates, along with 95% uncertainties were obtained for 172 of the TAFI sites (Table 2). Previously-obtained radiometric dates are available for 88 additional flows, with another approximately 60 flows from sections in the Aleutians, for which section ages, and stratigraphic information are reported. Ages were assigned to the remaining sites based on absolute and relative age data provided in the original TAFI publications. In some cases only the polarity chron is known, and a median chron age, with uncertainties corresponding to half the chron length were assigned. Thus assignments of age and age uncertainty (direct radiometric, relative stratigraphic, or chron) have been made for all TAFI sites. 873 sites have ages less than 5 Ma, the majority are of Brunhes (67%) or Matuyama (26%) age (Figure 4).

2:1 Paleomagnetic Field Procedures and Laboratory Methods

Sampling was restricted to lava flows or thin dikes – units that cool quickly, and can record the instantaneous geomagnetic field at the time and location of emplacement of the volcanic unit. Standard 1-inch-diameter paleomagnetic cores, about 4 inches long, were drilled in the field. Each site was determined to be in situ; post-emplacement tilting was avoided. Outcrops were surveyed using a magnetic compass and / or a Bartington magnetometer to minimize sampling of units subjected to lightning strikes. For each study, as many sites were sampled as possible during the field season, with a goal of at least 10 sites for a given polarity. On average, about 50 sites were obtained per study (Table 2). A minimum of 10 cores were drilled over a several-meter-extent of outcrop to allow assessment of orientation error at each site. (The data set from La Palma [*Tauxe et al.*, 2000] preceded these standards and 5–12 samples per site were drilled.) Each sample was oriented using a magnetic compass, and where possible a sun compass and/or back-sighting (see *Tauxe et al.*, 2003 for details). At high latitudes, when sun was unavailable and diurnal variations in declination can be large, a portable differential GPS was used to provide a reference baseline at each sites that was linked to individual core samples by sighting with a laser.

Laboratory methods vary slightly among studies, but a set of minimum criteria were adopted: In all cases natural remanent magnetizations were measured for all specimens, and one specimen per core for at least 5 distinct cores (samples), was subjected to stepwise alternating field or thermal demagnetization. Accompanying rock magnetic measurements, such as susceptibility and Curie temperature were also made. New $^{40}Ar/^{39}Ar$ radiometric ages were obtained for lava flows from ten studies. Details of the paleomagnetic and age measurements, and resulting data for each study are given in the original publications of paleomagnetic results [*Brown*, 2002; *Brown et al.*, 2004; *Johnson et al.*, 1998; *Mejia et al.*, 2002; *Mejia et al.*, 2004, *Mejia et al.*, 2005; *Opdyke & Musgrave*, 2005; *Opdyke et al.*, 2006; *Stone & Layer*, 2006; *Tauxe et al.*, 2000; *Tauxe et al.*, 2003; *Tauxe et al.*, 2004a; *Tauxe et al.*, 2004b]. In this paper we use site mean directions as follows. Original data, including all laboratory and field measurements, from the Azores [*Johnson et al.*, 1998], La Palma [*Tauxe et al.*, 2000], Southern Patagonia [*Mejia et al.*, 2004], Antarctica [*Tauxe et al.*, 2004a], Snake River [*Tauxe et al.*, 2004b], San Francisco Volcanics [*Tauxe et al.*, 2003], and Costa Rica [*Constable et al.*, in prep] have been archived in the MagIC database [*Solheid et al.*, 2002; http://www.earthref.org/MAGIC/]. Sample-level directions reported in MagIC use principal component analysis and require at least 4 demagnetization steps and a maximum angular deviation of the data about the stable component of less than 5°. Fisher mean directions were computed for all sites with at least 3 samples per site. Over 95% of these sites have site mean directions derived from at least 5 samples. For all other studies – Aleutians [*Stone and Layer*, 2006], Nunivak [*Coe et al.*, 2000], British Columbia [*Mejia et al.*, 2002], Mexico [*Mejia et al.*, 2005], Atacama and Tatara San Pedro [*Brown*, in prep], Easter Island [*Brown*, 2002], Patagonia [*Brown et al.*, 2004] – we have used the site mean directions reported in the original publication. In this paper we use only paleodirections, since absolute paleointensity mesurements are still underway for several of the TAFI studies.

2:2 Assessment of TAFI Data Quality

As has been discussed extensively (*e.g.*, *McElhinny and McFadden* [1997]; *Johnson & Constable* [1996]; *Merrill et al.*[1996]), assessment of data quality is critical to accurate identification of paleosecular variation and of non-GAD time-averaged field structure. Typically site mean directions with an associated α_{95} greater than (or k less than) a certain value are excluded from analyses. Recent regional data compilations consist of several hundred site mean directions, and enable an assessment of the behavior of TAF and PSV estimates as increasingly stringent data quality requirements are imposed. We use such an approach, as reported in *Tauxe et al.* [2003; hereafter *T03*] and by *Lawrence et al.* [2006; hereafter *L06*].

Our measure of data quality for individual sites is k. We use inclination anomaly, ΔI, (equation (3)) to characterize the TAF, and between-site VGP dispersion, S_B, (equation (4)), for PSV. We calculate ΔI and S_B using site mean directions with values of k greater than a cut-off value, denoted by k_{cut}. Increasingly stringent data quality criteria correspond to successively larger values of k_{cut}. The approach is discussed in detail in *L06* and we do not repeat it here. The TAFI data set differs from those in *T03* and *L06*, having sites from a broad range of latitudes, and we expect both PSV and TAF estimates to include a latitudinal signature. We investigate the TAFI data set by binning data from similar latitudes, but retain a distinction between northern and southern latitudes. Sufficient data are available at latitudes of approximately 50°N, 35°N, 25°S, 35°S, and 50°S to perform an investigation of how ΔI and S_B vary with k_{cut}. The results are shown in Figure 5 for normal polarity data only, since these dominate our data set. Normal polarity is defined here as site mean directions that have a corresponding positive VGP latitude – thus no distinction between stable polarity and transitional data is made in the evaluation of data quality.

Taken together, these regional analyses indicate that inclination anomaly is quite robust with respect to data quality, especially in regions with large data sets. For example, the latitude band with the most data, centered on 35°S, shows an average inclination anomaly that is small ($\approx 2°$) and positive, and does not change significantly as the value of k_{cut} is varied. For other regions, there is some change in the estimate of ΔI at high values of k_{cut} because the smaller data sets yield less reliable results. The behavior of S_B with k_{cut} varies from region to region. Overall, S_B is more sensitive to low quality data. All latitude bands except 35°S show a decrease in S_B of 2°–6° at values of k_{cut} around 40–90. This behavior corresponds to the removal of sites with directions further from the mean than the remainder of the population. These low quality data can result in overestimates of VGP dispersion. Our current data set is not able to resolve any latitudinal trend in this bias. For latitudes 50°S, 25°S, 35°N, values of k_{cut} of 250 or more result in noisy estimates of S_b due to the small number of data retained. Analysis of reverse polarity TAFI data showed similar behavior as a function of k_{cut}, although estimates of both S_B and ΔI display more scatter due to the much smaller data sets.

We also evaluated the principal components of the resulting distribution of directions for each value of k_{cut}, to investigate any changes in symmetry of the distributions with data quality (see *T03* for a discussion of this approach). We do not show the results here, since they do not provide any additional insight. For most data sets, the presence of some low-k sites does not change any symmetries (or lack of!) in the distributions of directions. For the TAFI data sets shown here, only data from Patagonia appear circularly symmetric.

2:3 The TAFI Data Set

The TAFI data set is summarized in Figure 6 on a study-by-study basis – transitional directions are excluded, and sites with $k \leq 100$ are distinguished (green) from those with $k > 100$ (blue). We exclude transitional directions, defined as directions with corresponding absolute values of VGP latitude less than 45°. This approach has traditionally been justified as a means of characterizing stable polarity average field geometry and its paleosecular variation, but it is important to recognize that it may well prejudice our view of the phenomena we want to study. There is no guarantee that a stable polarity geometry exists and, even if it did, it would in all likelihood be characterized by VGP distributions that vary with location. Ideally we would include all so-called transitional data, but geomagnetic reversals are an attractive target for study

so that in some regions the most disturbed field states would end up being over-represented. Excluding transitional directions avoids this non-uniformity in temporal sampling. We conservatively consider only sites with $k > 100$ for further analyses. In several cases, this results in discarding more data than seems necessary (Figures 5 and 6); however the choice provides consistency with other studies of regional data sets [*Tauxe et al.*, 2003; *Tauxe et al.*, 2004b; *Lawrence et al.*, 2006] and ensures that low quality data do not bias estimates of S_B (Figure 5). After removal of low-k and low-VGP-latitude sites, our TAFI data contribute 691 sites. Small mean inclination anomalies are observed in some studies, and on average reverse polarity fields show greater deviation from GAD (Figure 6 and see publications reporting individual study paleomagnetic results).

3. Additional Data

We supplement the TAFI data with eight regional data sets based on compilations from the literature; consequently these are more heterogeneous in associated age information, sampling and laboratory procedures than our TAFI data set. Six of the compilations have been described elsewhere: paleomagnetic directions from the NW and SW USA [*Tauxe et al.*, 2004b and 2003 respectively], Mexico [*Mejia et al.*, 2005; *Lawrence et al.*, 2006], Hawaii, the South Pacific and Reunion [*Lawrence et al.*, 2006]. We add new data sets for New Zealand and Japan, and summarize these here. Sampling in both Japan and New Zealand has been concentrated on Brunhes or Matuyama age outcrops, and so we investigate these polarity periods only. Paleomagnetic and age data reported in all studies contributing to the regional compilations are available from the MagIC database at EarthRef.org(www.earthref.org/MAGIC).

The volcanic centers of the North Island, New Zealand have been extensively sampled for studies of paleosecular variation, beginning with *Cox* [1969, 1970]. Our compilation includes paleodirections from all sites, except those suspected of tectonic rotation and those with fewer than 3 samples. The latter criterion ensures that for each site we are able to make an estimate of within-site error. Our data set comprises 140 sites of Brunhes or Matuyama age – flows, dikes, welded tuffs, welded ignimbrites or small domes (Table 3; Figures 7a,b). In many studies, radiometric dates were obtained for several of the flows sampled for paleomagnetic purposes. We use directional and age data from sites from the Auckland province [*Shibuya et al.*, 1992], South Auckland province [*Briggs et al.*, 1994], Northland [*Shibuya et al.*, 1995], and the Taupo Volcanic Zone [*Shane et al.* 1994; *Tanaka et al.*, 1996; *Tanaka et al.*. 1997]. We take care to avoid samples from the Mamaku ignimbrite, since the origin of anomalous directions from this exposure is debated [*Shane et al.* 1994; *Black et al.*, 1996].

Our data set for Japan comprises 176 sites, of which 172 are Brunhes age (Table 4; Figures 7c,d). As with the New Zealand data set, many of the paleomagnetic studies also report new radiometric dates. The regional tectonics is complicated with block rotations likely affecting some areas including the Izu Peninsula [*Kikawa et al.*, 1989], and we take care not to include such sites. Notably, we do not include here the studies of [*Kono*, 1968; 1971] that were included in our previous global PSV data compilation [*Johnson & Constable*, 1996]. It is possible that some of these sites are tectonically affected. Furthermore, other, more recent studies provide paleomagnetic directions at nearby sites, and use modern laboratory methods.

We conducted an assessment of data quality for these new compilations. Estimates of ΔI were found to be robust for all values of k_{cut}. Estimates of PSV are robust for values of k_{cut} up to about 250 (beyond which there are insufficient data to assess PSV), and give $S_B \approx 16^\circ$. Thus, as for the TAFI data we only consider sites with $k > 100$ in our further investigations.

Paleodirections from all contributing sites are shown in Figures 7b and 7d. For New Zealand, 92 Brunhes-age stable polarity sites have $k > 100$. The distribution of these directions is non-Fisherian (Figure 7b) – the mean inclination is compatible with that predicted by GAD, but a significant positive declination anomaly is observed (Table 3). Of the 26 Matuyama sites, 16 have a value of k greater than 100, and the resulting mean direction is compatible with GAD (Table 3). For Japan, 97 Brunhes-age sites have $k > 100$. The distribution of directions is non-Fisherian, with a mean direction indistinguishable from GAD (Table 4).

4. Toward a New Global Data Compilation: Latitudinal Variations in the TAF and PSV

We combine our TAFI data set with the new compilations from Japan and New Zealand, and previously published compilations for the SW USA [*Tauxe et al.*, 2003], the NW USA [*Tauxe et al.*, 2004b], and 20° latitude [*Lawrence et al.*, 2006]. We retain sites with at least 3 samples (note that our TAFI data set contains mostly sites with at least 5 samples per site), values of k greater than 100 and VGP latitudes higher than 45°. This results in a data set of 2283 (D, I) pairs, compared with 314 (D, I) pairs meeting both these criteria and the *DMAG 4* criteria of *MM97*. The new data set supercedes and replaces all of the *MM97 DMAG 4* sites, except those from Iceland, and spans latitudes from 78°S to 53°N. In particular, the TAFI data significantly improve coverage in the southern hemisphere. This was previously restricted to 3 locations – Tahiti, Reunion and New Zealand (Table 1), for which the numbers of data have been greatly increased (Table 5) – and now includes TAFI data from 8 additional locations (Table 2). Site level age information is available for all the regional compilations except that from the SW USA [*Tauxe et al.*, 2003] – in that study sites with ages less than 5 Ma were retained, but age information is only reported for those sites dated radiometrically. (Numbers reported in Table 1 reflect sites with age information.) Examination of the temporal distribution of our data set (Figure 8 and Table 2) shows that sampling is concentrated in the Brunhes, but suggests there are also sufficient data to examine behavior during the Matuyama epoch.

The new data set although still not global in distribution, overwhelms previous compilations in number, quality and age constraints, and substantially improves geographical coverage and temporal sampling of the Brunhes and Matuyama epochs. Because there are gaps in data coverage (*e.g.*, Europe) we do not address the issue of longitudinal structure in field behavior; rather we use this data set to investigate latitudinal variations in the TAF and PSV.

We divide our data set into latitudinal bands, governed by the distribution of sampling sites. Latitude bands are no more than $\pm 5°$ in spatial extent. The total number of 0 – 5 Ma sites in each latitude bin varies from 21 to 897 (Table 6). We use ΔI and S_B as measures of the TAF and PSV respectively. In estimating ΔI, we account for variations in site latitude within a given latitude band as follows. From the observed (D, I) we compute the direction (D', I') relative to the expected GAD direction at the site. The mean inclination anomaly is computed from the unit vector average of the (D', I') in a given latitude band, and plotted at the mean latitude. S_B is calculated using equation (4). The 95% confidence limits on both ΔI and S_B are calculated using a bootstrap resampling technique. We analyze the Brunhes and Matuyama epochs separately, and the combined normal and reverse polarity data for the 0–5 Ma period. (Normal and reverse data are combined by using the antipode of the reverse polarity directions.). As most data are of Brunhes or Matuyama age we do not perform plate motion corrections.

The results for ΔI are shown in Figure 9 and Table 6. The best geographical coverage is provided by the 0–5 Ma combined data set. Latitude bands with more than 50 sites have 95% confidence intervals about the mean inclination anomaly of less than $\pm 2°$ for the 0–5 Ma (and Brunhes) period. Northern / southern hemisphere asymmetry is evident, with negative mean inclination anomalies of up to 5° at low latitudes, and extending to mid-northern latitudes (40°N). Elsewhere, zero, or small positive, inclination anomalies are observed. The 0–5 Ma signal may in part reflect averaging of different normal and reverse polarity signals. This is substantiated by the quite different Brunhes and Matuyama epoch inclination anomaly profiles.

For each data set in Figure 7 we perform a grid search to find the best-fitting two parameter zonal field model to the inclination anomalies. We explore a parameter space in which the g_2^0 and g_3^0 terms can vary from -50% to 50% of the g_1^0 term, in increments of 1%. For each (g_2^0, g_3^0) pair we calculate the weighted root mean square misfit of the predicted inclination anomaly to the observed inclination anomaly. (The weights are determined by the 95% confidence intervals). The best fitting models are provided in Table 7. The Brunhes inclination anomalies are best fit by $g_2^0 = .02 g_1^0$ and $g_3^0 = .01 g_1^0$, a result that is similar to previous zonal models for global Brunhes data sets [*Johnson & Constable*, 1995; 1997; *Merrill et al.*, 1996; *Carlut & Courtillot* 1998]. The larger amplitude Matuyama inclination anomalies are best fit by both larger axial quadrupole and axial octupole terms, with $g_2^0 = .04 g_1^0$ and $g_3^0 = .05 g_1^0$. Larger amplitude inclination

anomalies during reverse polarity periods have long been noted, although their cause (geomagnetic versus rock magnetic – see *e.g.Merrill et al.* [1996]) has been debated. Large octupole contributions during reverse polarity periods have also been suggested by recent high quality data sets [*Opdyke et al.*, 2006]. The 0 – 5 Ma combined normal and reverse polarity data are fit by a two parameter model in which g_2^0 = .04g_1^0 and g_3^0 = .03g_1^0. Note that the octupole term here is smaller than that obtained by *Lawrence et al* [2006] for two reasons. First the data set used here supercedes that of *Lawrence et al* [2006]; the majority of sites are the same but there are some differences, notably the inclusion of the New Zealand and Japanese data. Second, here we find a best fitting two-parameter model to the mean inclination anomaly, weighted by the uncertainties in the mean, whereas *Lawrence et al.* [2006] fit the site level inclination data.

It has long been known [*Creer*, 1983] that biased estimates of direction are obtained when unit vectors are averaged. The bias is manifest as deviations of inclination from GAD predictions that are well approximated by a zonal octupole contribution. We assess the plausible magnitude of such a signal in our data set using a statistical model for PSV [*Constable & Johnson*, 1999]. The TAF structure in the simulations is prescribed as purely g_1^0 (*i.e.*the time-averaged value of all other spherical harmonic terms is set to zero), and PSV is given by the statistics of the spherical harmonic coefficients prescribed in *Constable & Johnson* [1999]. We simulate directions at our observed site locations, by drawing n samples per site from a Fisherian distribution, with a Fisher precision parameter given by the observed within-site k. The mean inclination is computed for a given latitude band in the same way as for our data. Averaging of unit vectors produces an apparent inclination anomaly versus latitude signature that is best fit (using the grid search algorithm described above) by a g_2^0=0.0 term, and g_3^0= .02 g_1^0. The same result is obtained if we use the statistical model of *Tauxe & Kent* [2004]. If the observed inclination anomalies are corrected for this bias, then the g_3^0 contributions for the Brunhes, Matuyama, and 0–5 Ma data sets are reduced in amplitude to -.01g_1^0, .02g_1^0 and .01g_1^0 respectively. Uncertainties in the magnitude of the bias exist because existing paleosecular variation models do not adequately fit regional distributions of PSV data [*Constable & Johnson*, 1999; *Tauxe & Kent*, 2004; *Lawrence et al.*, 2006].

VGP dispersion for the Brunhes, Matuyama and 0–5 Ma data sets is shown in Figure 10 (values are given in Table 6), and compared with predictions from two paleosecular variation models: Model G [*McFadden et al.*, 1988] and TK03 [*Tauxe & Kent*, 2004]. The TK03 predictions assume a TAF specified by GAD, and 10,000 simulations were made at latitude increments of 5°. For the combined 0–5 Ma data set, good agreement of the data with Model G, and in particular, TK03, is seen at mid northern (20° to 50°) and mid southern (20° to 40°) latitudes. S_B for data sets from Ecuador, Costa Rica, and the South Pacific is higher than model predictions. For the South Pacific, this results from the presence of several transitions in the data set, that remain evident even when the lowest VGP latitude data are excluded (our cut-off of 45°). Estimates of S_B at Costa Rica and Ecuador may be influenced by the small sample size – additional data are clearly required to better estimate PSV at low latitudes. The 0–5 Ma data set from Patagonia (two TAFI studies combined – see Table 2) results in an estimate of S_B that is large – this is due to scatter in directions from Gauss and Gilbert age flows. Brunhes age data display little variation in S_B versus latitude in the northern hemisphere; the only exception is low secular variation at 20°N that results from the Hawaiian data set [*Lawrence et al.*, 2006]. The Matuyama data set shows several estimates of S_B that are higher than during the Brunhes. This difference in S_B between normal and reverse polarity epochs has been observed many times previously and its origin is still not understood [*McElhinny et al.*, 1996].

5. Summary and Conclusions

The TAFI project has resulted in a new high quality set of paleodirections from lava flows, suitable for studying the TAF and PSV. Data from 17 locations provide significantly enhanced spatial coverage over previous data sets [*Quidelleur et al.*, 1994; *Johnson & Constable*, 1996] and over the highest quality data ('*DMAG 4*') present in the compilation of *MM97*. The TAFI data set comprises 873 paleodirections in the 0–5 Ma time interval, with most data of Brunhes and Matuyama age (Figure 4 and Table 5). In addition, data collection efforts by other groups has enabled the compilation of eight regional data sets [*Tauxe et al.* 2003; *Tauxe et al.* 2004; *Lawrence et al.*, 2006; this study], which supercede and replace all but one of the

locations of DMAG 4 data (Tables 1 and 5).

The resulting combined data set allows investigation of the TAF and PSV as a function of latitude. Investigations of data quality indicate that estimates of S_B and ΔI are reliable for values of $k > 100$ at the site level. As the TAFI sampling efforts focussed on collecting data from stable polarity epochs, we exclude transitional data from our analyses. This allows direct comparison of our data set with earlier studies of PSV and the TAF during stable polarity periods. The temporal data distribution means that it is now possible to compare the TAF and PSV during the Brunhes and Matuyama epochs, as well as investigating combined normal and reverse data for 0–5 Ma.

The large numbers of data from several latitudes results in smaller uncertainties in ΔI and S_B than previously [*e.g.*, *Johnson & Constable*, 1995; 1997]. We have conducted a grid search to find best-fitting 2-parameter zonal models for the time-averaged field structure. These models indicate axial quadrupole contributions to the TAF of 2% – 4% of the axial dipole term (Figure 9 and Table 7), compatible with previous studies [*Johnson & Constable*, 1995; 1997; *Carlut & Courtillot*, 1998; *Merrill et al.*, 1996]. Substantial axial octupole contributions (3% to 5%) are found for the Matuyama epoch and the 0–5 Ma data set. However, simulations using statistical models for PSV [*Johnson & Constable*, 1999; *Tauxe et al.*, 2004] suggest a g_3^0 signature on the order of 2% is attributable to the bias incurred by the averaging of unit vectors.

Evaluations of VGP dispersion from our new data set show only modest agreement with existing PSV models (Figure 10). Large uncertainties in S_B are seen when the number of sites is less than 50, and simulations suggest that several hundred sites are needed to adequately estimate PSV [*Tauxe et al.*, 2003]. Differences between S_B at the same locations are observed for the Brunhes and Matuyama epochs. As the source of these differences is unclear, interpretation of S_B for field behavior is perhaps best confined to the Brunhes epoch. Surprisingly, this data set indicates little variation of S_B with latitude, the exception being low PSV at Hawaii.

The new data set is not complete globally. Existing data from Europe, Iceland, and other recent studies still need to be incorporated and it is clear from the results presented here that additional data are needed from several places (notably equatorial and low latitudes) to allow even latitudinal trends in the TAF and PSV to be properly characterized. In this paper we have only considered zonal structure in the field, although it is evident from the 20° latitude compilation of *Lawrence et al.* [2006] and from estimates of ΔI and S_B from the TAFI studies that there are regional differences in the TAF and PSV from data sets at similar latitudes. Rather than excluding lower quality and / or excursional data, future studies can use more sophisticated weighting schemes to allow the incorporation of all observations. In regions where large data sets are available, progress can be made through inversions of regional data sets for TAF and PSV statistics.

Increasing numbers of high quality absolute intensity measurements, along with time series of relative paleointensity and inclination from sediments means that in the near future it should be possible to combine these disparate data types into more comprehensive models for field behavior. Such studies will require careful internal assessment of each contributing data type. Assessment of one such data type – paleodirections from volcanics – has been reported here, and shows that the combined data collection efforts of the paleomagnetic community over the past decade have resulted in dramatic improvements in spatial and temporal coverage of 0 – 5 Ma geomagnetic field behavior.

6. Acknowledgements

This work was supported under NSF grants EAR-9805164 (Tauxe), and NSF EAR0337712 (C. Johnson and C. Constable). We thank Kristin Lawrence and Vicky Mejia for input on the 20° latitude regional compilation.

7. Figure Captions

Figure 1: Time-averaged radial magnetic field, (B_r), at the core-mantle boundary (CMB), on different time scales. Units are μT. (a) Historical Field: 1590 - 1990, Model GUFM1 [*Jackson et al.*., 2000], (b) Archeo-Field: 0 - 7 ka, Model CALS7K.2 [*Korte & Constable*, 2005] , (c) Paleo-Field: 0 - 5 Ma, axial dipole plus axial quadrupole field (see text), (d) Model LSN1 [*Johnson & Constable*, 1997] (e) Model LN1 [*Johnson & Constable*, 1995].

Figure 2: Declination (a), (c), (e) and inclination (b), (d), (f) anomalies in degrees (deviations from GAD direction) at Earth's surface predicted from models for the three time intervals in Figure 1: (a) and (b) Model GUFM1, (c) and (d) CALS7K.2, (e) and (f) Model LSN1. The scale bar for the historical field is twice that for the archeo-field, and four times that for paleofield anomalies.

Figure 3: Locations of TAFI sites (red circles) and regional compilations from literature (blue stars: *Tauxe et al.* [2003]; *Tauxe et al.* [2004b]; *Lawrence et al.* [2006]; this study). Open circle denotes Spitzbergen site, where data are mostly older than 5 Ma and not reported here.

Figure 4: Age distribution for the 873 TAFI sites with ages less than 5 Ma. Average age and an estimate of error in the age are obtained via (a) radiometric dates obtained as part of the TAFI project (172 flows), (b) previous radiometric ages made directly on TAFI sites (88 flows) (c) radiometric dating of stratigraphic section (3 sections, 60 flows), (c) inferred age – stratigraphy and/or polarity chron ($\approx$ 500 flows).

Figure 5: Inclination anomaly (ΔI) and VGP dispersion (S_B) versus cut-off value of k (k_{cut}) for five latitude bins of the TAFI data set. Normal polarity data only are shown. Mean ΔI, S_B (blue) along with the bootstrap 95% confidence intervals (red) are shown. Green curve indicates number of contributing data at each value of k_{cut}.

Figure 6: Equal area projections of site directions for each of the 17 TAFI studies. Closed (open) circles represent projections onto the lower (upper) hemisphere. Sites with estimates of the within-site Fisher precision parameter $k \leq 100$ are shown in green, those with $k > 100$ are shown in blue. Transitional field directions (VGP latitudes less than 45°) have been excluded. The GAD field direction at the mean site location is given by the red triangle. North is 0° declination.

Figure 7: New Zealand (a,b) and Japanese (c,d) data compilations. Age distributions of contributing sites are shown in (a) – New Zealand, and (b) – Japan. Equal area projections (figure format as in figure 6) of site directions are shown in (c) – New Zealand and (d) – Japan.

Figure 8: Age distribution for the combined data set of 2283 pairs of declination and inclination measurements (TAFI data plus regional compilations) used in this study.

Figure 9: Inclination anomaly versus latitude for latitudinally binned data (triangles) with 95% confidence intervals (error bars), and best-fit 2-parameter zonal field model (solid line). (a) 0–5 Ma data set, normal and reverse data combined, (b) Brunhes-age normal polarity data, (c) Matuyama-age reverse polarity data. Numbers of data in each bin are indicated.

Figure 10: VGP dispersion, S_b (degrees) versus latitude for (a) 0–5 Ma data set, normal and reverse data combined; (b) Brunhes-age normal polarity data; (c) Matuyama-age reverse polarity data. For reference predicted dispersion for Model G [*McFadden et al.*, 1998] (dashed line) and TK03 [*Tauxe & Kent*, 2004] (solid) are shown.

Table 1: DMAG 4 data of *McElhinny & McFadden,* 1997

Region	N	Replaced?	New reference
New Zealand	56	Yes	This compilation (Table 3)
Japan	21	Yes	This compilation (Table 4)
Reunion	27	Yes	*Lawrence et al.*, 2006
Tahiti	135	Yes	*Lawrence et al.*, 2006
SW USA	54	Yes	*Tauxe et al.*, 2003
NW USA	41	Yes	*Tauxe et al.*, 2004b
Canaries	13	Yes	*Tauxe et al.*, 2000
Iceland	47	No	–
Total	394		

Legend: Previously reported data of adequate quality for TAF /PSV modeling [*McElhinny et al.*, 1997]. N is total number of *DMAG 4* data from region (no selection based on k or α_{95}). Last 2 columns indicate whether these data sets have been superceded.

Table 2: TAFI Studies

Region	λ (°)	ϕ (°)	N_{total}	N_{dated}	Reference
Aleutians	54.4	190.1	89	0	*Stone & Layer*, 2006
Nunivak	53.0	-172.0	56	0	*Coe et al.*, 2000
British Columbia	51.5	-122.4	53	0	*Mejia et al.*, 2002
Snake River	43.0	- 113.5	26	21	*Tauxe et al.*, 2004b
San Francisco Volc.	35.3	-111.9	37	0	*Tauxe et al.*, 2003
Azores	37.8	-25.4	35	12	*Johnson et al.*, 1998
La Palma	28.8	-17.9	26	8	*Tauxe et al.*, 2000
Mexico	20.1	-99.7	16	7	*Mejia et al.*, 2005
Costa Rica	10.2	-84.4	31	18	*Constable et al.*, in prep.
Ecuador	-0.4	-78.3	53	11	*Opdyke et al.*, 2006
Atacama	-23.3	-67.7	46	23	*Brown et al.*, in prep.
Easter Island	-27.1	-109.2	62	0	*Brown*, 2002
Chile	-36.0	-70.9	193	0	*Brown*, in prep.
Australia	-37.7	144.2	38	0	*Opdyke & Musgrave*, 2005
Patagonia	-47.0	-71.1	36	34	*Brown*, in prep
Patagonia	-51.2	-70.6	50	20	*Mejia et al.*, 2004
McMurdo	-78.1	165.4	36	18	*Tauxe et al.*, 2004a
17 studies total			883	172	

Legend: *Region* – geographical area of study; λ – mean study latitude in degrees (positive north); ϕ – mean study longitude in degrees (positive east); N_{total} – total number of sites with declination and inclination measurement pairs; N_{dated} – number of sites for which new radiometric (usually $^{40}Ar/^{39}Ar$) dates were obtained; *Reference* – publication in which the paleomagnetic study is reported.

Table 3: New Zealand Studies

Location	λ (°)	ϕ (°)	N_{Bru}	N_{Mat}	Reference
Auckland volcanic province	-36.9	174.8	17	–	Shibuya *et al.*, 1992
South Auckland volcanic province	-37.2	174.9	7	10	Briggs *et al.*, 1994
Taupo ignimbrites[1]	-38.5	176.5	15	–	Shane *et al.*, 1994
Northland	-35.4	174.0	9	2	Shibuya *et al.*, 1995
Central Taupo[2,3]	-38.5	176.0	39	14	Tanaka *et al.*, 1996
Taupo, Ruapehu volcano[3]	-39.3	175.6	27	–	Tanaka *et al.*, 1997
Total			114	26	

Brunhes (sites with k>100) $N = 92$ $D = 8.1°$ $I = -56.8°$ $\alpha_{95} = 2.1°$ $I_{GAD} = -57.5°$
Matuyama (sites with k>100) $N = 16$ $D = 180.3°$ $I = 61.3°$ $\alpha_{95} = 5.8°$ $I_{GAD} = 57.5°$

Legend: λ – mean study latitude in degrees; ϕ – mean study longitude in degrees; N_{Bru}, N_{Mat} – number of Brunhes / Matuyama sites retained (see text). [1] Mamaku ignimbrite excluded since reported directions are anomalous and not well understood; [2] directions from Lake Whakamura are excluded since post emplacement tectonics reported; [3] directions supercede and replace those of *Cox* [1969; 1971]

Table 4: Japan Studies

Location	λ (°)	ϕ (°)	$N_{Brunhes}$	$N_{Matuyama}$	Reference
Higshi-Izu volcano group	34.0	138.0	28	–	Heki, 1983
Ashitaka dikes	35.2	138.8	35	–	Tsunakawa & Hamano, 1988
Ashitaka volcano & Izu-Oshima Isl[1]	35.9	147.5	48	–	Kikawa *et al.*, 1989
Mt. Fuji & Mt. Oshima	32.0	131.5	6	–	Tanaka, 1990
Goto Islands, Tsushima Strait	32.9	128.9	5	–	Ishikawa & Tagami, 1991
Zao volcanic group[2]	38.1	140.5	11	4	Otake *et al.*, 1993
Daisen volcano, Shikotsu caldera	35.4	138.6	6	–	Tanaka *et al.*, 1994
Ontake Volcano	35.0	139.0	33	–	Tanaka & Kobayashi, 2003
Total			172	4	

Brunhes (sites with k>100) $N = 97$ $D = 358.7°$ $I = 54.3°$ $\alpha_{95} = 2.5°$ $I_{GAD} = 54.9°$

Legend: Table format as in Table 3. [1] excluded sites from Izu peninsula due to possible tectonic rotation; [2] excluded site ZK03, since of Jaramillo age

Table 5: Numbers of data used in this study

Compilation	N_{total}	N_{used}	N_{Bru}	N_{Mat}	N_{Gau}	N_{Gil}	Reference
TAFI [1]	873	677^{691}	465^{465}	168^{179}	30^{32}	14^{15}	This paper
Japan	172	97	97	–	–	–	This paper
New Zealand	140	108	92	16	–	–	This paper
Hawaii	895	765	293	66	243	163	*Lawrence et al.*, 2006
Mexico	325	132	49	46	29	8	*Lawrence et al.*, 2006
South Pacific	482	284	1	228	41	14	*Lawrence et al.*, 2006
Reunion	144	84	64	20	–	–	*Lawrence et al.*, 2006
N. W. USA	92	78	62	11	3	2	*Tauxe et al.*, 2004
S. W. USA	678	58	33	13	3	9	*Tauxe et al.*, 2003
Totals	3801	2283	1156	568	349	210	

Legend: *Compilation*: data compilation reported in *Reference*; N_{total} – total number of 0–5M̃a data available with at least 3 samples per site (5 for TAFI compilation); N_{used} denotes all data meeting our additional selection criteria (sites with k < 100 and VGP latitude less than 45°); N_{Bru} – Brunhes, N_{Mat} – Matuyama, N_{Gau} – Gauss, and N_{Gil} Gilbert age. [1] Note that new data from Mexico, collected as part of the TAFI project are included in the summary numbers for Mexican compilation here, and the TAFI summary numbers have been corrected accordingly (the uncorrected numbers are given in the superscript).

Table 6: Summary Statistics vs. Latitude

$\bar{\lambda}$ (°)	N_{Bru}	ΔI_{lo}^{hi}	$S_b{}_{lo}^{hi}$	N_{Mat}	ΔI_{lo}^{hi}	$S_b{}_{lo}^{hi}$	N_{total}	ΔI_{lo}^{hi}	$S_b{}_{lo}^{hi}$
-78.1	27	$-1.5^{1.7}_{-4.8}$	$20.6^{24.7}_{16.1}$	6	$1.2^{4.1}_{-7.5}$	$26.6^{33.1}_{18.8}$	34	$-1.0^{1.8}_{-4.1}$	$21.1^{24.6}_{17.1}$
-49.5	20	$-2.5^{2.4}_{-7.4}$	$21.6^{25.1}_{17.6}$	14	$0.2^{5.1}_{-4.5}$	$19.9^{25.2}_{14.7}$	59	$0.2^{2.8}_{-2.4}$	$24.3^{36.5}_{22.3}$
-36.9	234	$2.1^{3.5}_{0.9}$	$16.6^{17.8}_{15.1}$	38	$0.6^{4.1}_{-2.5}$	$13.5^{14.5}_{10.9}$	287	$1.5^{2.7}_{0.3}$	$16.0^{17.2}_{14.7}$
-22.7	124	$-2.7^{-1.2}_{-4.6}$	$14.3^{16.3}_{12.5}$	19	$6.1^{12.6}_{-2.2}$	$17.5^{20.6}_{14.4}$	169	$-2.3^{-0.6}_{-4.3}$	$15.2^{16.7}_{13.7}$
-17.2	–	–	–	100	$-0.7^{3.0}_{-4.4}$	$19.5^{22.1}_{17.2}$	362	$0.4^{2.4}_{-1.8}$	$18.2^{19.7}_{16.7}$
-0.4	10	$-9.4^{-0.8}_{-18.0}$	$16.9^{20.4}_{13.0}$	15	$-3.7^{1.6}_{-9.9}$	$16.8^{23.4}_{11.8}$	27	$-5.2^{-1.0}_{-10.3}$	$15.9^{20.2}_{12.6}$
10.2	19	$-2.5^{4.8}_{-11.3}$	$16.3^{20.6}_{12.3}$	–	–	–	27	$-4.2^{2.1}_{-12.7}$	$17.3^{22.3}_{12.7}$
20.4	339	$-3.3^{-2.2}_{-4.4}$	$11.5^{12.7}_{10.4}$	51	$-5.5^{-1.9}_{-8.6}$	$14.8^{18.3}_{11.4}$	897	$-6.0^{-5.1}_{-6.9}$	$14.8^{15.4}_{14.0}$
28.8	7	$-3.0^{2.9}_{-12.9}$	$15.7^{22.1}_{10.0}$	12	$-7.9^{-5.9}_{-14.4}$	$16.2^{19.6}_{13.5}$	21	$-4.9^{-1.5}_{-10.3}$	$15.8^{18.3}_{13.0}$
36.1	160	$-1.8^{-0.1}_{-3.5}$	$15.6^{17.0}_{14.3}$	31	$-6.8^{-2.8}_{-9.8}$	$15.4^{17.7}_{12.8}$	208	$-3.3^{-1.6}_{-5.1}$	$16.1^{17.4}_{14.9}$
44.8	72	$-0.6^{1.7}_{-2.8}$	$15.6^{16.9}_{14.0}$	7	$-3.1^{2.9}_{-5.8}$	$17.3^{21.7}_{11.6}$	99	$-1.2^{0.6}_{-3.0}$	$15.0^{16.4}_{13.8}$
52.7	135	$1.7^{3.2}_{0.7}$	$15.7^{17.0}_{14.1}$	23	$6.2^{11.4}_{1.6}$	$26.6^{33.1}_{18.8}$	172	$1.9^{3.1}_{0.7}$	$17.7^{19.2}_{16.3}$

Legend: λ – mean latitude in degrees; N_{Bru}, N_{Mat}, N_{total} – number of Brunhes-age normal polarity, Matuyama-age reverse polarity, or 0–5M̃a normal and reverse polarity data combined. ΔI_{lo}^{hi}, $S_b{}_{lo}^{hi}$ are the inclination anomaly and between-site VGP dispersion in degrees, along with their 95% confidence limits.

Table 7: Best-Fitting Zonal TAF Models

Time Period	$G_2^0 = g_2^0/g_1^0$	$G_3^0 = g_3^0/g_1^0$
Brunhes	0.02	0.01
Matuyama	0.04	0.05
0–5 Ma combined	0.02	0.03

8. REFERENCES

Black *et al.*, 1996. xxxxx. , , .

Bloxham, J. *et al.*, 1989. Geomagnetic secular variation. *Phil. Trans. Roy. Soc. London, A*, **329**, 415–502.

Bloxham, J. & A. Jackson, 1992. Time-dependent mapping of the magnetic field at the core-mantle boundary. *J. Geophys. Res.*, **97**, 19,537–19,563.

Brown, L., 2002. Paleosecular variation from Easter Island revisited: modern demagnetization of a 1970s data set. *Phys. Earth Planet. Inter.*, **133**, 73-81.

Brown, L. L., Singer, B. S., and Gorring, M., 2004. Paleomagnetic and Geochronologic Results from Mesita del Lago Buenos Aires, Patagonia. *G-Cubed*, **5**, doi:10.1029/2003GC000526.

Briggs, R. M., Okada,T., Itaya,T., Shibuya,H., & I. E. M. Smith, 1994. K-Ar ages, paleomagnetism, and geochemistry of the South Auckland volcanic field, North Island, New Zealand. *New Zealand J. Geol. Geophys.*, **37**, 143-153.

Carlut, J. & V. Courtillot, 1998. How complex is the time-averaged geomagnetic field over the last 5 million years?. *Geophys. J. Int.*, **134**, 527–544.

Christensen, U.R., & P. Olson, 2003. Secular variaiton in numerical geodynamo models with lateral variations of boundary heat flow. *Physics Earth Planet. Int.*, **138**, 39–54.

Constable, C.G., & C.L.Johnson, 1999. Anisotropic paleosecular variation models: Implications for geomagnetic observables. *Phys. Earth Planet. Inter.*, **115**, 35–51.

Coe, R. S., X. Zhao, J. J. Lyons, C. J. Pluhar & E. A. Mankinen , 2000. Revisiting the 1964 collection of Nunivak lava flows. *EOS Trans AGU*, **81**, Fall Meeting Supp. Abstract # GP62A-06.

Cox, A., 1969. A paleomagnetic study of secular variation in New Zealand. *Earth Planet. Sci. Lett.*, **6**, 257–267.

Cox, A., 1971. Remanent magnetization and susceptibility of late Cenozoic rocks from New Zealand. *New Zealand J. Geol. Geophys.*, **14**, 192–207.

Creer, K. M., 1962. The dispersion of the geomagnetic field due to secular variation and its determination from remote times from paleomagnetic data. *J. Geophys. Res.*, **67**, 3461–3476.

Creer, K. M., 1983. Computer synthesis of geomagnetic paleosecular variations. *Nature*, **304**, 695–699.

Glatzmaier *et al.*, 1999. xxxx. , , .

Gubbins, D., & P. Kelly, 1993. Persistent patterns in the geomagnetic field over the past 2.5 Myr. *Nature*, **365**, 829–832.

Heki, K., 1983. Paleomagnetic study of the Higashi-Izu Volcano Group and pyroclastics flow deposits in Kagoshima Prefecture: paleosecular variation during the last 40,000 years. *J. Geomag. Geolect.*, **35**, 383-390.

Ishikawa,N. & T. Tagami, 1991. Paleomagnetism and fission-track geochronology on the Goto and Tsushima Islands in the Tsushima Strait area: implications for the opening mode of the Japan Sea. *J. Geomag.*

Geoelect., **43**, 229-253.

Hollerbach & Jones, 1993a,b. xxxxx. *xxxx*, **xxxx**, xxxx.

Hulot, G., C. Eymin, B. Langlais, M. Mandea & N. Olsen, 2002. Small-scale structure of the geodynamo inferred from Oersted and Magsat satellite data. *Nature*, **416**, 620–623.

Jackson, A., A. R. T. Jonkers, & M. R. Walker, 2000. Four centuries of geomagnetic secular variation from historical records. *Phil. Trans. Roy. Soc. London, Series A*, **358**, 957–990.

Johnson, C. L. & C. G. Constable, 1995. The time-averaged geomagnetic field as recorded by lava flows over the past 5 Myr. *Geophys. J. Int.*, **122**, 489–519.

Johnson, C. L. & C. G. Constable, 1996. Paleosecular variation recorded by lava flows over the last 5 Myr. *Phil. Trans. Roy. Soc. London, Series A, A*, **354**, 89–141.

Johnson, C. L. & C. G. Constable, 1997. The Time-Averaged Geomagnetic Field: Global and Regional Biases for 0-5 Ma. *Geophys. J. Int.*, **131**, 643–666.

Johnson, C.L., J. R. Wijbrans, C. G. Constable, J. Gee, H. Staudigel, L. Tauxe, V.-H. Forjaz, M. Salgueiro, 1998. $^{40}Ar/^{39}Ar$ ages and paleomagnetism of São Miguel lavas, Azores. *Earth Planet. Sci. Lett.*, **160**, 637–649.

Kelly, P. & D. Gubbins, 1996. The geomagnetic field over the past 5 Myr. *Geophys. J. Int.*, **128**, 315–330.

Kikawa, E., Koyama,M., Kinoshita,H., 1989. Paleomagnetism of Quaternary volcanics in the Izu Peninsula and adjacent areas, Japan, and its tectonic significance. *J. Geomag. Geoelect.*, **41**, 175-201.

Kokhlov, A., G. Hulot & J. Carlut, 2001. Towards a self-consistent approach to palaeomagnetic field modelling. *Geophys. J. Int.*, **145**, 157-171.

Kono, M., 1968. Paleomagnetism of Pleistocene Usami Volcano, Izu Peninsula, Japan - Intensity of the Earth's magnetic field in geological time II. *J. Geomag. Geoelect.*, **20**, 353-366.

Kono, M., 1971. Intensity of the Earth's magnetic field in geological time III. Pleistocene and Pliocene data from Japanese volcanic rocks. *J. Geomag. Geoelect.*, **23**, 1-9.

Kono, M., & P.H. Roberts, 2002. Recent Geodynamo simulations and observations of the geomagnetic field. *Rev. Geophys.*, , 10.1029/2000RG000102.

Korte, M., and C.G. Constable, 2005. Continuous geomagnetic models for the past 7 millennia II: CALS7K. *Geochem. Geophys. Geosyst.*, **6(2)**, Q02H16 DOI 10.1029/2004GC000801.

Lawrence, K., C. G. Constable & C. L. Johnson, 2006. Paleosecular Variation and the average geomagnetic field at $\pm 20^\circ$ latitude. *Geol., Geochem., Geosystems*, **7**, doi:10.1029/2005GC001181.

Lee, S., 1983. A study of the time-averaged paleomagnetic field for the past 195 million years. *Phd Thesis*, Australian National University.

McElhinny, M. W., McFadden, P. L., & R. T. Merrill, 1996. The time averaged paleomagnetic field 0 – 5 Ma. *J. Geophys. Res.*, **101**, 25007-25027.

McElhinny, M.W. and McFadden, P.L., 1997. Palaeosecular variation over the past 5 Myr based on a new

generalized database. *Geophys. J. Int.*, **131**, 240-252.

McElhinny M. W. & R. T. Merrill, 1975. Geomagnetic secular variation over the past 5 my.. *Rev. Geophys. Space Phys.*, **13**, 687–708.

McFadden, P.L., 2004. Is 600 Myr long enough for the random paleogeographic test of the geomagnetic axial dipole assumption?. *Geophys. J. Int.*, **158**, 443–445.

McFadden, P.L., Merrill, R.T. & M.W. McElhinny, 1988. Dipole/quadrupole family modelling of paleosecular variation. *J. Geophys. Res.*, **93**, 11853–11588.

Merrill, R. T., M. W. McElhinny, & P. L. McFadden, 1996. *The Magnetic Field of the Earth: Paleomagnetism , the Core and the Deep Mantle*. Academic Press.

Mejia, V., R. W. Barendregt & N. D. Opdyke, 2002. Paleosecular variation of brunhes age lava flows from British Columbia, Canada. *Geochem. Geophys. Geosyst.*, **3(12)**, doi:10.1029/2002GC000353.

Mejia, V., N. D. Opdyke, J. F. Vilas, B. S. Singer & J. S. Stoner, 2004. Plio-Pleistocene time-averaged field in southern Patagonia recorded in lava flows. *Geochem. Geophys. Geosyst.*, **5(3)**, doi:10.1029/2003GC000633.

Mejia, V., H. Böhnel, N. D. Opdyke, M. A. Otega-Rivera, J. K. W. Lee & Aranda-Gomez, 2005. Paleosecular variation and time-averaged field recorded in late Pliocene-Holocene lava flows from Mexico. *Geochem. Geophys. Geosyst.*, **6(7)**, doi:10.1029/2004GC000871.

Olson, P. & J. Aurnou, 1999. A polar vortex in the Earth's core. *Nature*, **402**, 170–173.

Opdyke, N. & R. Musgrave, 2004. Paleomagnetic results from the Newer Volcanics of Victoria: Contribution to the Time Averaged Field Initiative. *Geochem. Geophys. Geosyst.*, **5(3)**, doi:10.1029/2003GC000632.

Opdyke, N., M. Hall, V. Mejia, K. Huang, & D. A. Foster, 2006. The time-averaged field at Ecuador: results from the equator. submitted to *Geochem. Geophys. Geosyst.*.

Otake,H., Tanaka,H., Kono,M., Saito,K., 1993. Paleomagnetic study of Pleistocene lavas and dikes of the Zao Volcanic Group, Japan. *J. Geomag. Geoelect.*, **45**, 595-612.

Quidelleur, X. *et al.*, 1994. Long-term geometry of the geomagnetic field for the last 5 million years; an updated secular variation database from volcanic sequences.. *Geophys. Res. Lett.*, **21**, 1639–1642.

Quidelleur, X., & V. Courtillot, (1996). On low degree spherical harmonic models of paleosecular variation. *Phys. Earth Planet. Inter.*, **95**, 55–77.

Shane, P., T. Black, & J. Westgate, 1994. Isothermal plateau fission-track age for a paleomagnetic excursion in the Mamaku Ignimbrite, New Zealand, and implications for late Quaternary stratigraphy. *Geophys. Res. Lett.*, **21**, 1695–1698.

Shibuya, H., Cassidy, J., Smith, I.E.M., Itaya, T., 1992. A geomagnetic excursion in the Brunhes epoch recorded in New Zealand basalts. *Earth Planet. Sci. Letters*, **111**, 41-48.

Shibuya, H., Cassidy, J., Smith, I.E.M., Itaya, T., 1995. Paleomagnetism of young New Zealand basalts and longitudinal distribution of paleosecular variation. *J. Geomag. Geoelect.*, **47**, 1011-1022.

Schneider, D. A. & D. V. Kent, 1990. The time-averaged paleomagnetic field. *Rev. Geophys.*, **28**, 71–96.

Solheid, P. Constable, C., Koppers, A., Jackson, M., Banerjee, S.,, 2002. Research-oriented Data Base for Rock and Paleomagnetism to Be Developed. *EOS Transactions, American Geophysical Union*, **83(48)**, 560.

Sreenivasan, B. & C. A. Jones, 2005. Structure and dynamics of the polar vortex in the Earth's core. *Geophys. Res. Lett.*, **32**, L20301.

Sreenivasan, B. & C. A. Jones, 2006. Azimuthal winds, convection and dynamo action in the polar regions of planetary cores. submitted to *Geophys. J. Int.*.

Stone, D. & P. Layer, 2006. Paleosecular variation and GAD studies of 0—2 Ma flow sequences from the Aleutian Islands, Alaska. *Geochem. Geophys. Geosyst.*, **7(4)**, doi:10.1029/2005GC001007.

Tanaka, H., Turner, G.M., Houghton, B.F., Tachibana, T., Kono, M., McWilliams, M.O., 1996. Palaeomagnetism and chronology of the central Taupo Volcanic Zone. *Geophys. J. Int.*, **124**, 919-934.

Tanaka, H., K. Kawamura, K, Nagao, & B.F. Houghton, 1997. K-Ar ages and paleosecular variation of direction and intensity from Quaternary lava sequences in the Ruapehu Volcano, New Zealand. *J. Geomagn. Geoelectr.*, **49**, 587–599.

Tanaka, H. *et al.*, 1994. Paleointensities for 10-22 ka from volcanic rocks in Japan and New Zealand. *Earth Planet. Sci. Lett.*, **122**, 29-42.

Tanaka, H. *et al.*, 1991. Paleomagnetism of the Shakotan Peninsula, West Hokkaido, Japan. *J. Geomag. Geoelect.*, **43**, 277-294. ???????????

Tsunakawa,H., Hamano,Y., 1988. Paleomagnetic study of the Ashitaka Dike Swarm in central Japan. *J. Geomag. Geoelect.*, **40**, 221-226.

Tauxe, L., H. Staudigel & J. Wijbrans, 2000. Paleomagnetism and $^{40}Ar/^{39}Ar$ ages from La Palma in the Canary Islands. *Geochem. Geophys. Geosyst.*, **1**, ISSN: 1525-2027.

Tauxe, L., C. Constable, C. L. Johnson, A. A. P. Koppers, W. R. Miller, and H. Staudigel, 2003. Paleomagnetism of the Southwestern USA recorded by 0-5Ma igneous rocks . *Geochem. Geophys. Geosyst.*, **4(4)**, 8802 , doi: 10.1029/2002GC000343.

Tauxe, L., Gans, P. & E. Mankinen, 2004a. Paleomagnetism and 40Ar /39Ar ages from volcanics extruded during the Matuyama and Brunhes Chrons near McMurdo Sound, Antarctica . *Geochem. Geophys. Geosyst.*, **5(6)**, doi:10.1029/2003GC000656.

Tauxe, L., Luskin, C. Selkin, P. Gans, P., & A. Calvert, 2004b. Paleomagnetic results from the Snake River Plain: Contribution to the time-averaged field global database. *Geochem. Geophys. Geosyst.*, **5(8)**, doi:10.1029/2003GC000661.

Tauxe, L. & D. Kent, 2004. A simplified statistical model for the geomagnetic field and the detection of shallow bias in paleomagnetic inclinations. Was the ancient magnetic field dipolar?. **In** "*Timescales of the Internal Geomagnetic Field*", ed. J.E.T.C. Channell, D.V. Kent, W. Lowrie, J.G. Meert, Geophysical Monograph Series 145, American Geophysical Union, pp. 10.1029/145GM07. 101–115

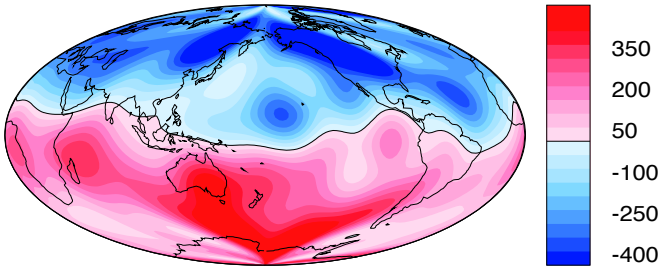

(a) Model GUFM1

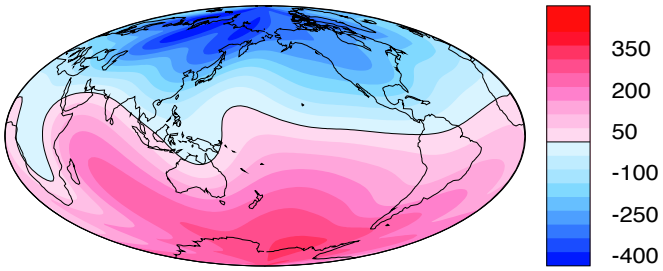

(b) Model CALS7K.2

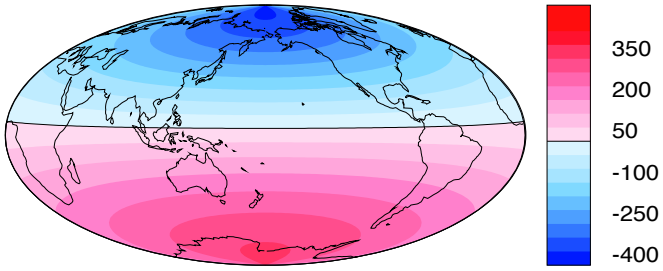

(c) Zonal field model

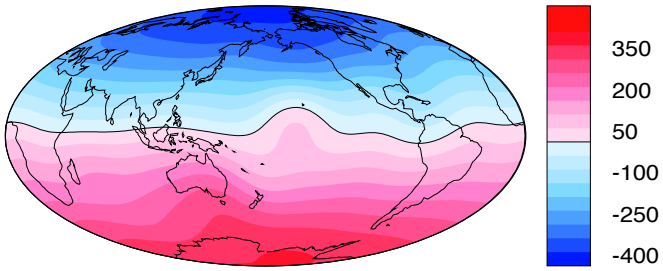

(d) Model LSN1

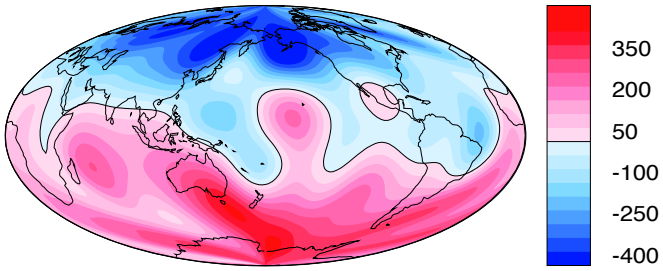

(e) Model LN1

Figure 1

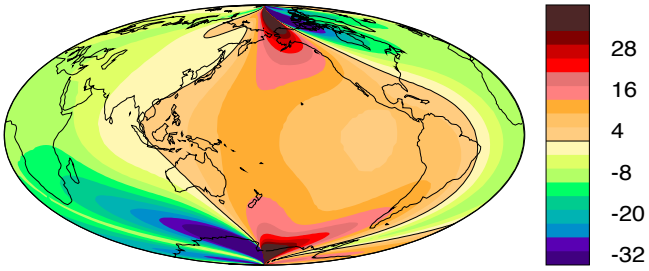

(a) GUFM Declination Anomaly

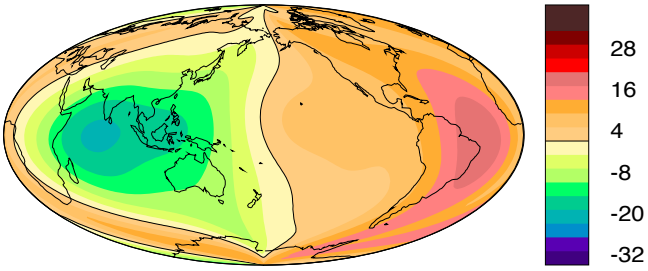

(b) GUFM Inclination Anomaly

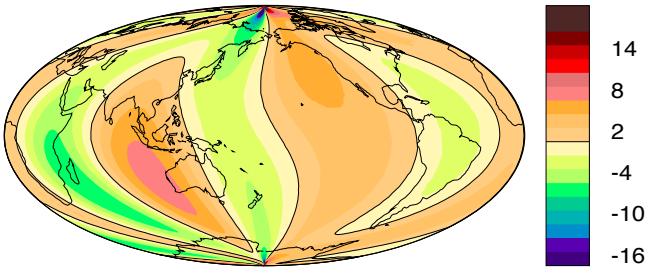

(c) CALS7K.2 Declination Anomaly

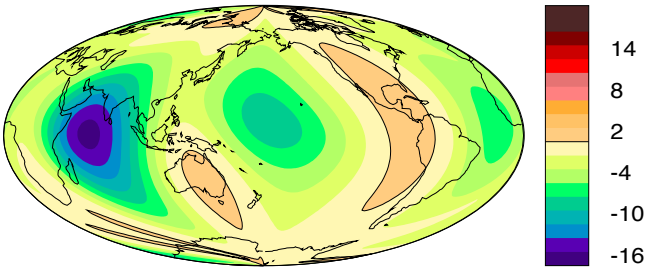

(d) CALS7K.2 Inclination Anomaly

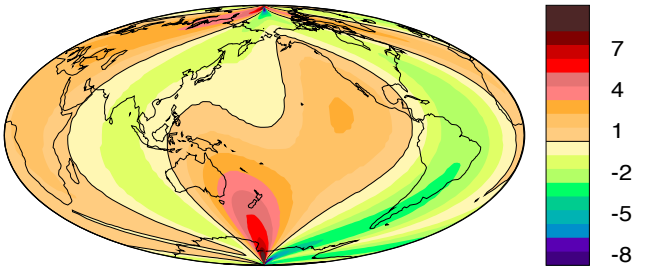

(e) LSN1 Declination Anomaly

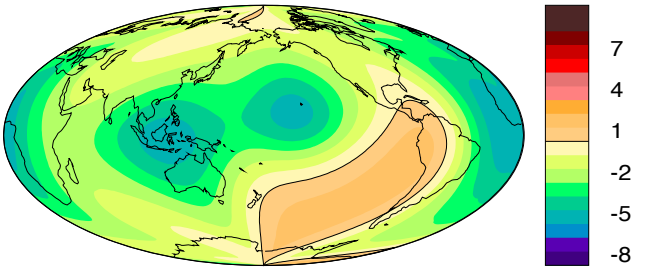

(f) LSN1 Inclination Anomaly

Figure 2

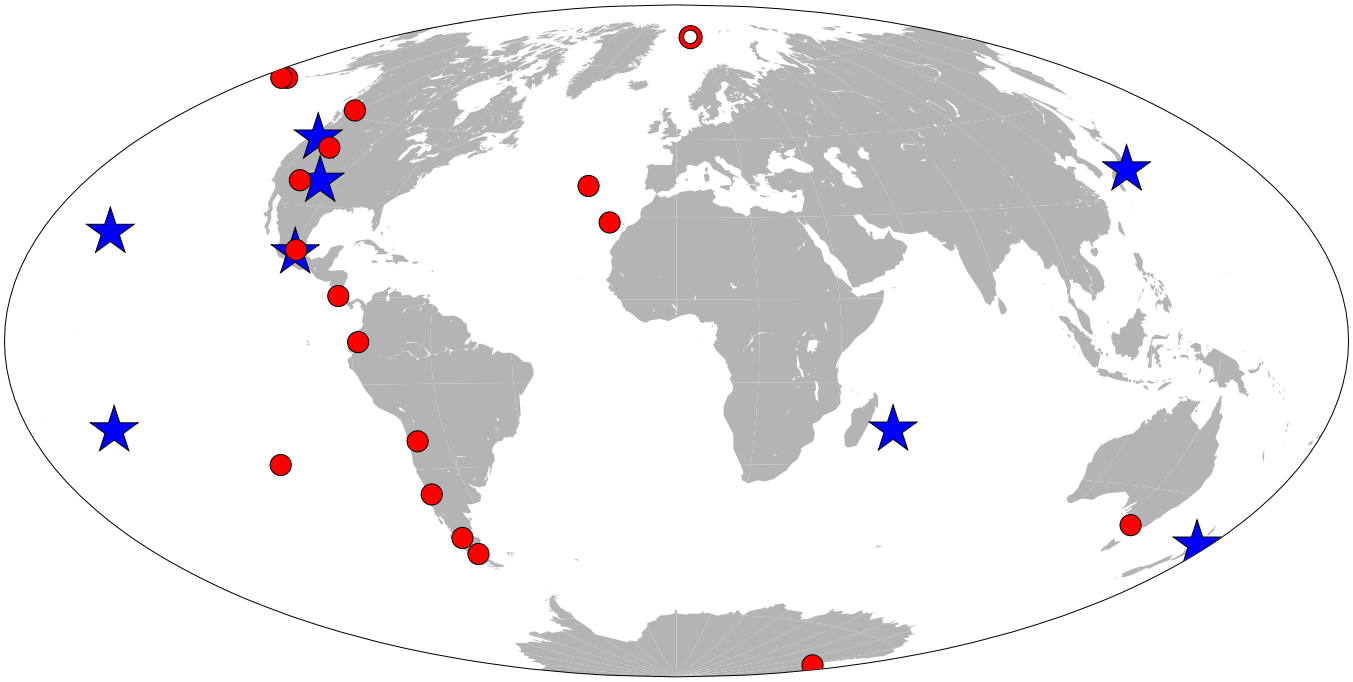

Figure 3

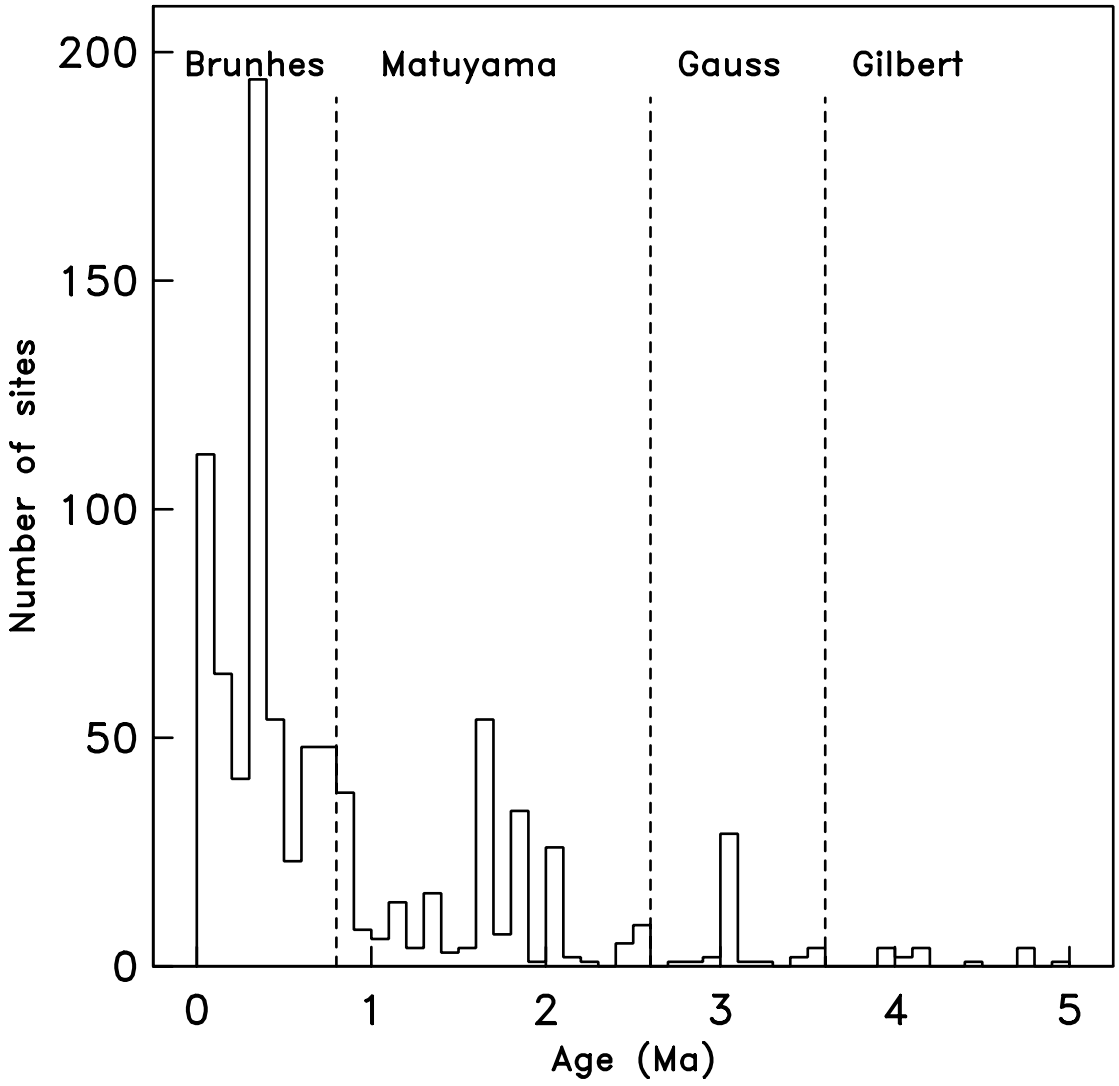
Brunhes
Matuyama
Gauss
Gilbert
200
150
100
50
0
Number of sites
0
1
2
3
4
5
Age (Ma)

Figure 4

(a) 50°N: British Columbia and Aleutians

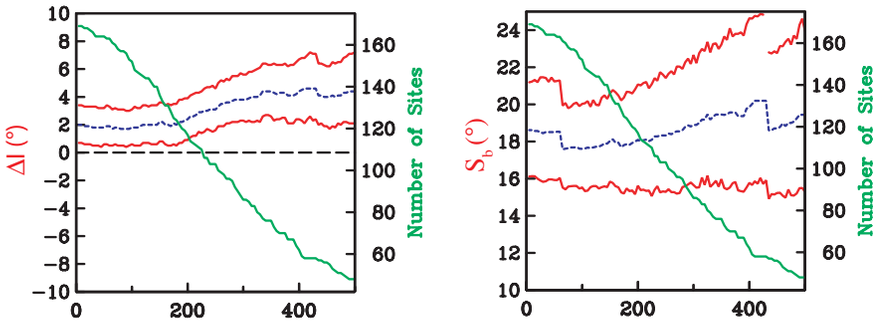

(b) 35°N: Azores and San Francisco Volcanics

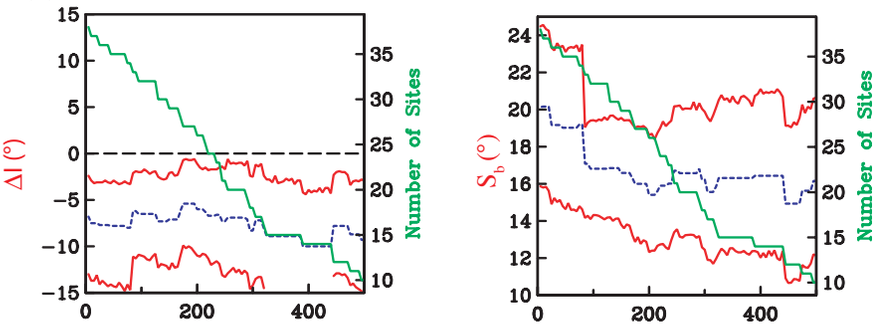

(c) 25°S: Easter Island and Atacama

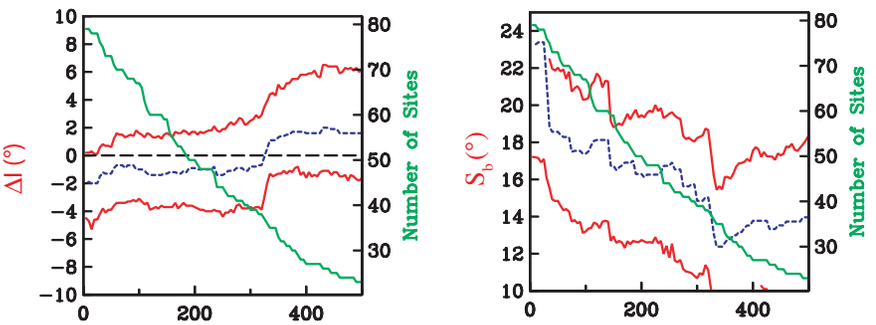

(d) 35°S: Tatara San Pedro and Australia

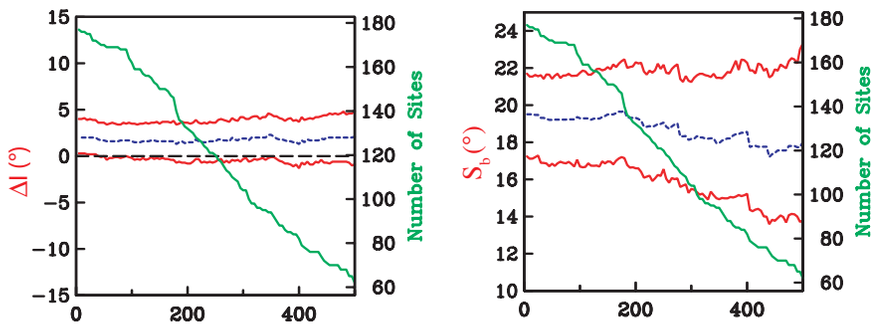

(e) 50°S: Patagonia

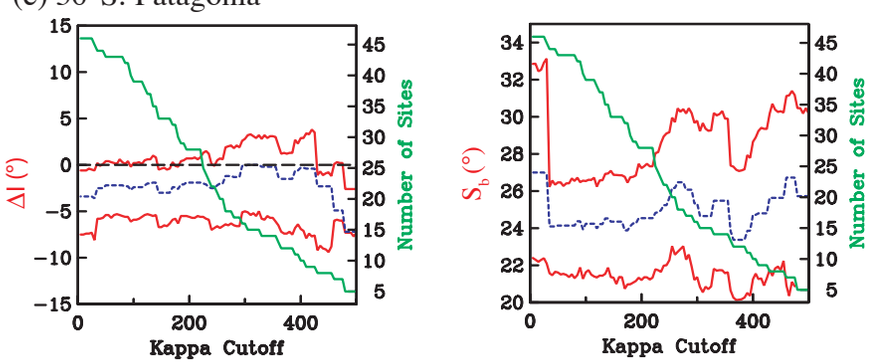

Figure 5

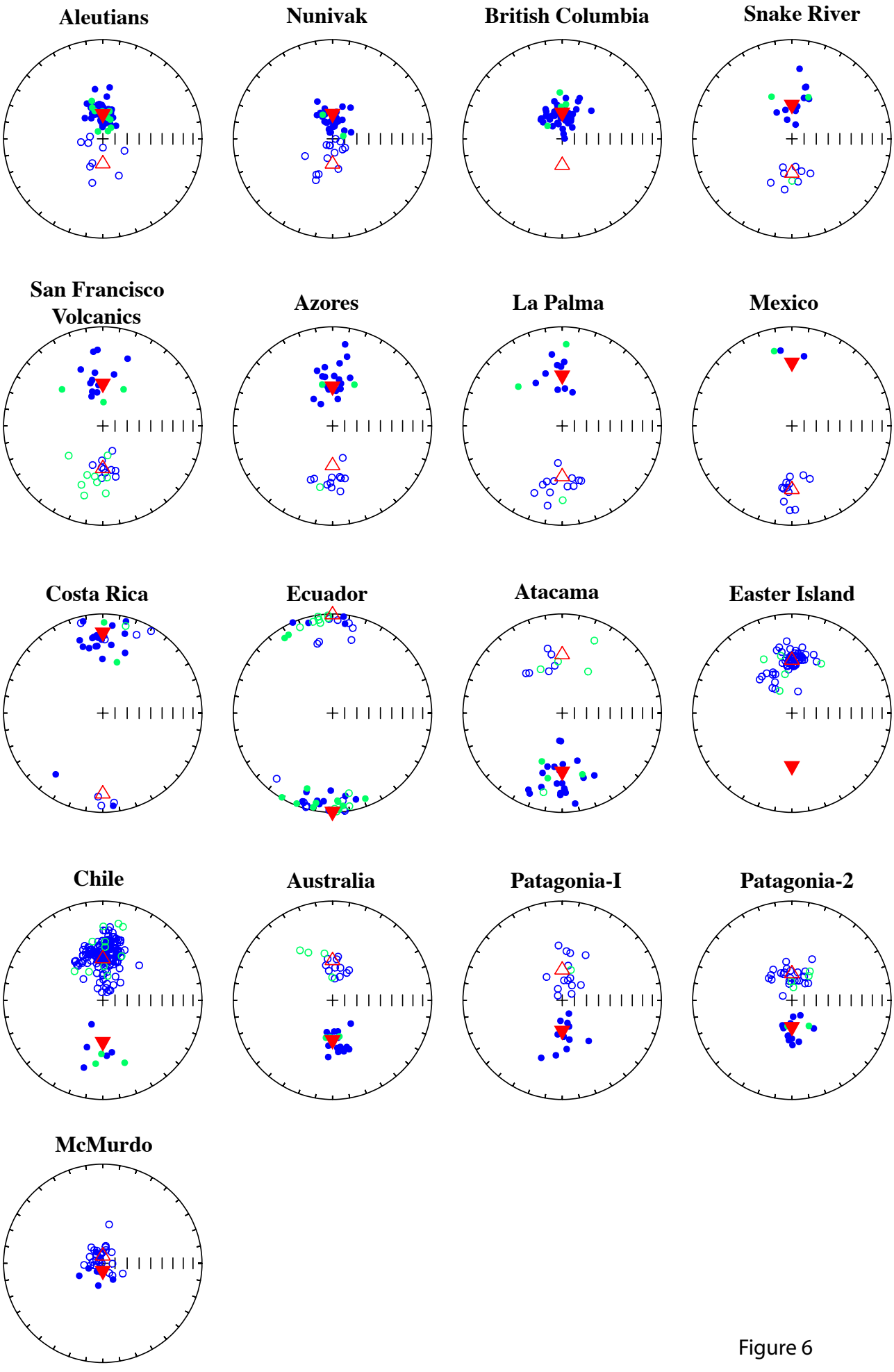
Aleutians
Nunivak
British Columbia
Snake River
San Francisco Volcanics
Azores
La Palma
Mexico
Costa Rica
Ecuador
Atacama
Easter Island
Chile
Australia
Patagonia-I
Patagonia-2
McMurdo

Figure 6

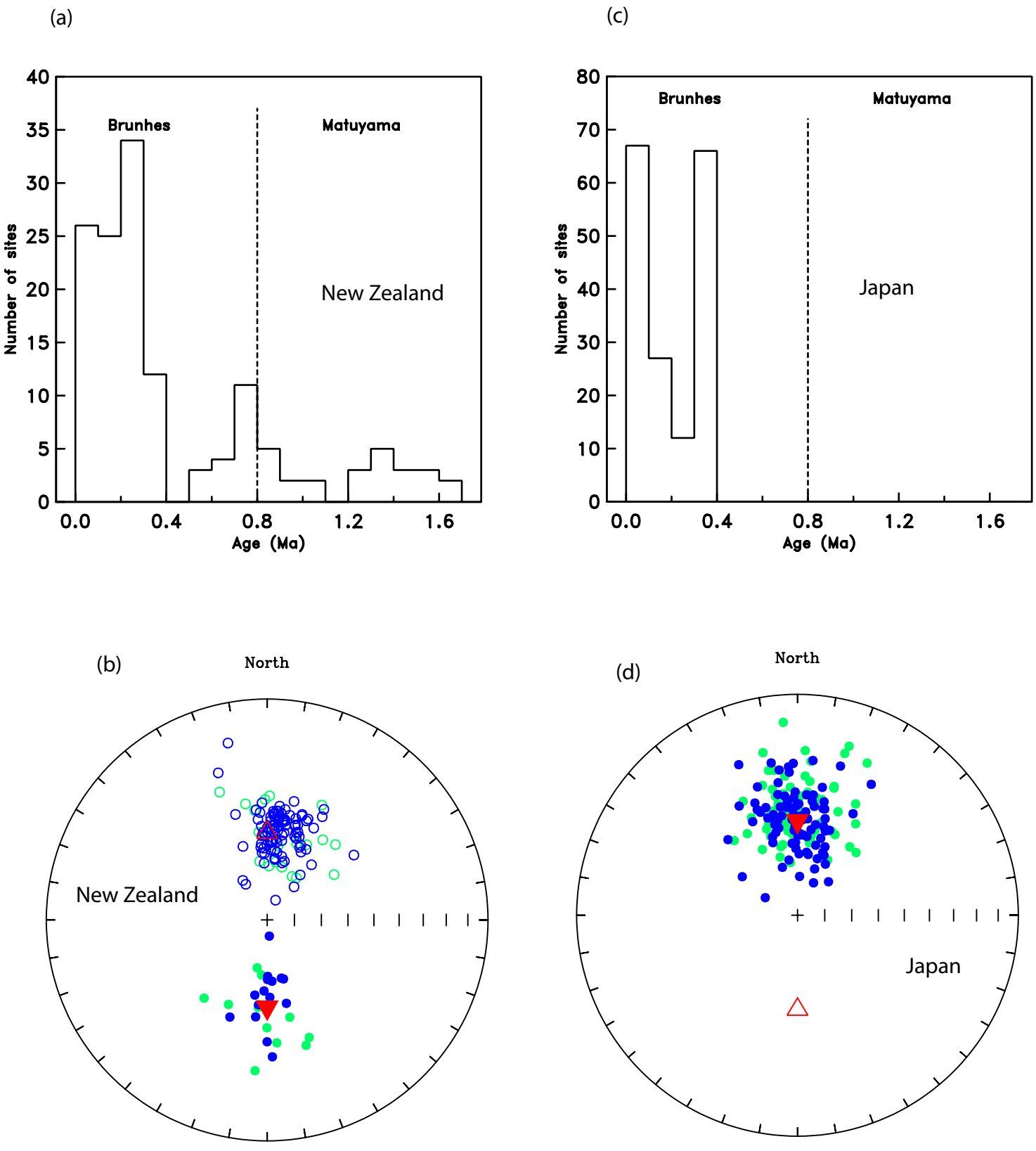
(a)
Brunhes
Matuyama
New Zealand
Number of sites
Age (Ma)
(c)
Brunhes
Matuyama
Japan
Number of sites
Age (Ma)
(b)
North
New Zealand
(d)
North
Japan

Figure 7

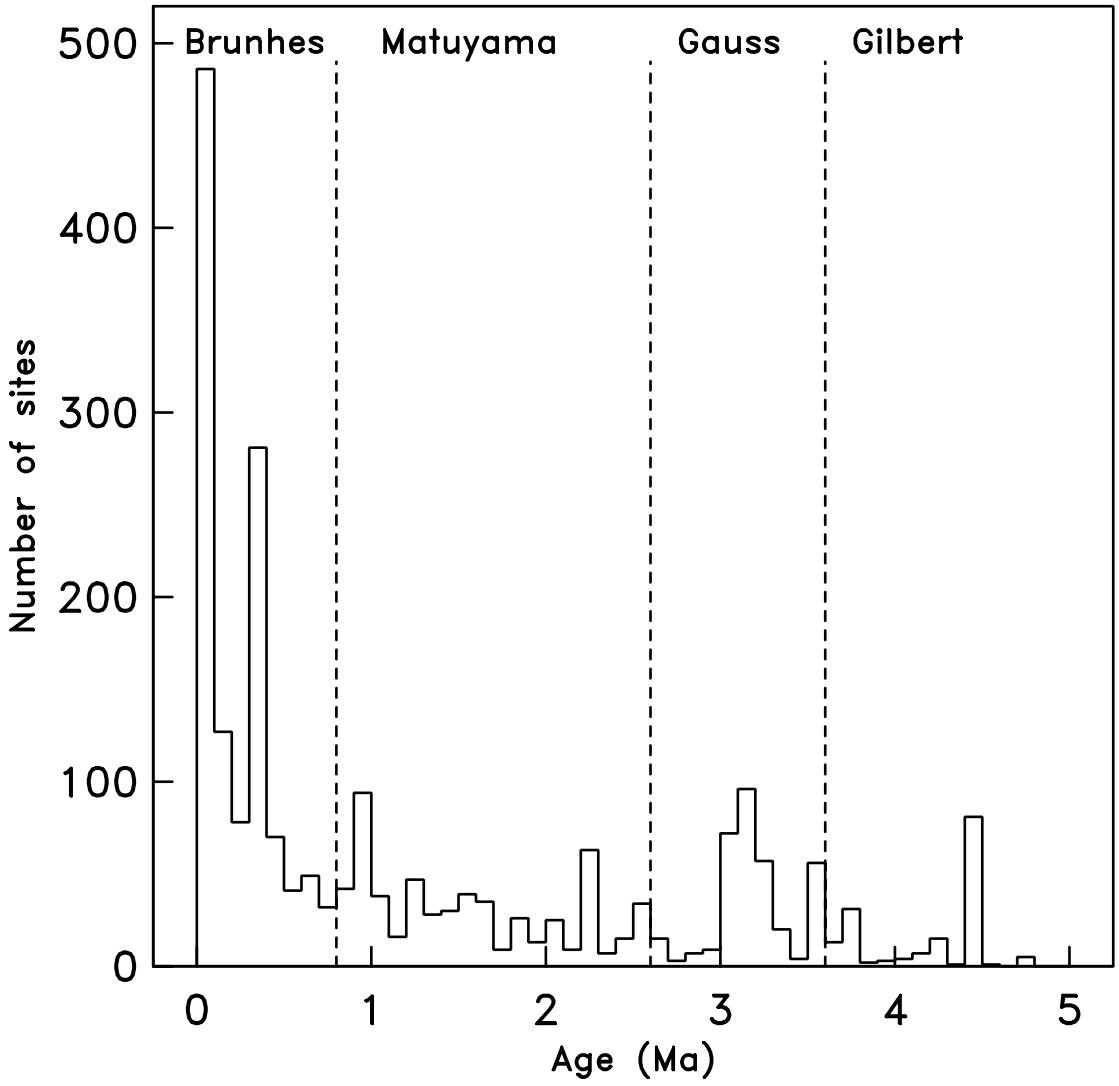
Brunhes
Matuyama
Gauss
Gilbert
500
400
300
200
100
0
Number of sites
0
1
2
3
4
5
Age (Ma)

Figure 8

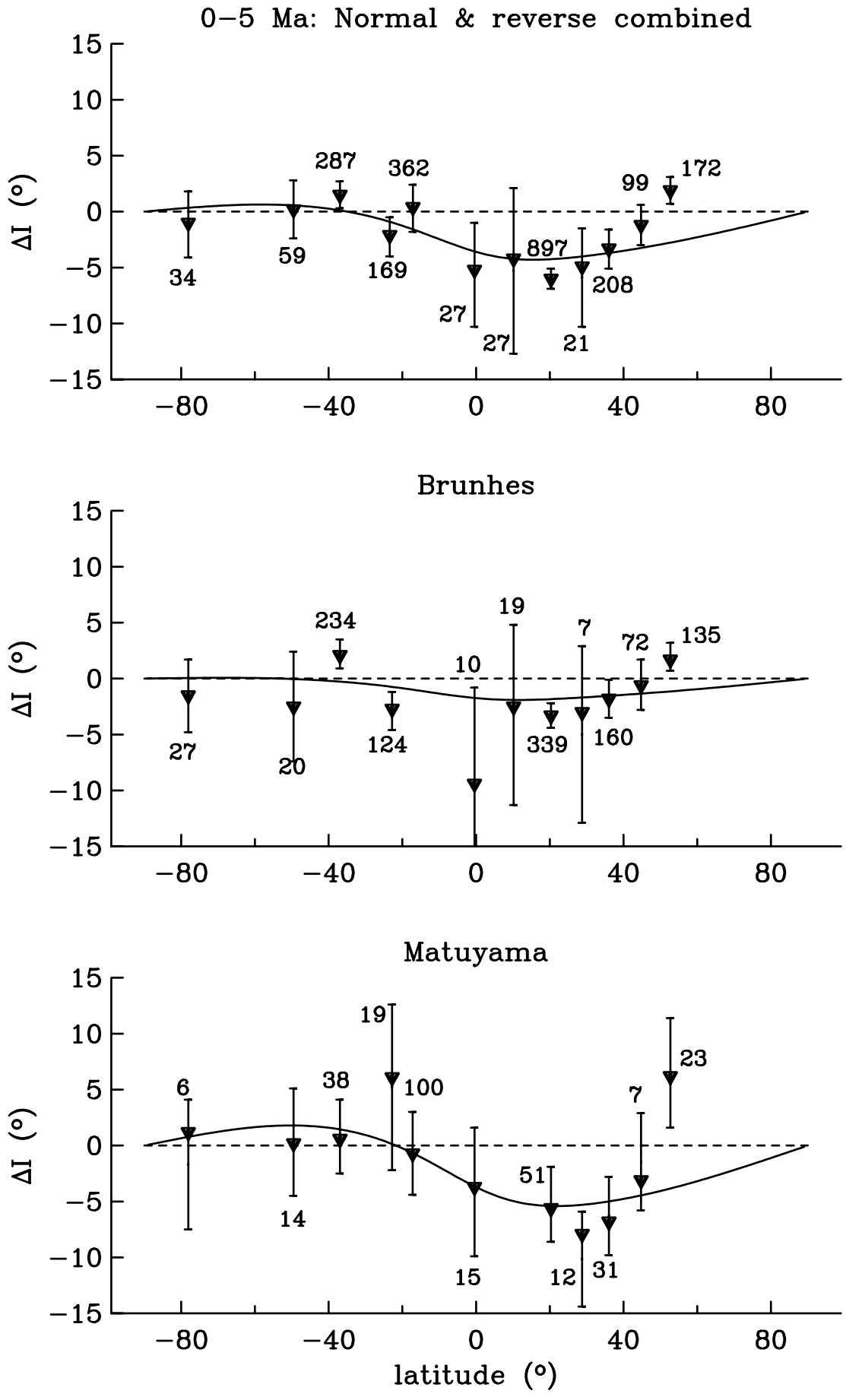
0–5 Ma: Normal & reverse combined
ΔI (°)
15
10
5
0
−5
−10
−15
−80
−40
0
40
80
34
59
287
169
362
27
27
897
21
208
99
172
Brunhes
27
20
234
124
10
19
339
7
160
72
135
Matuyama
6
14
38
19
100
15
51
12
31
7
23
latitude (°)

Figure 9

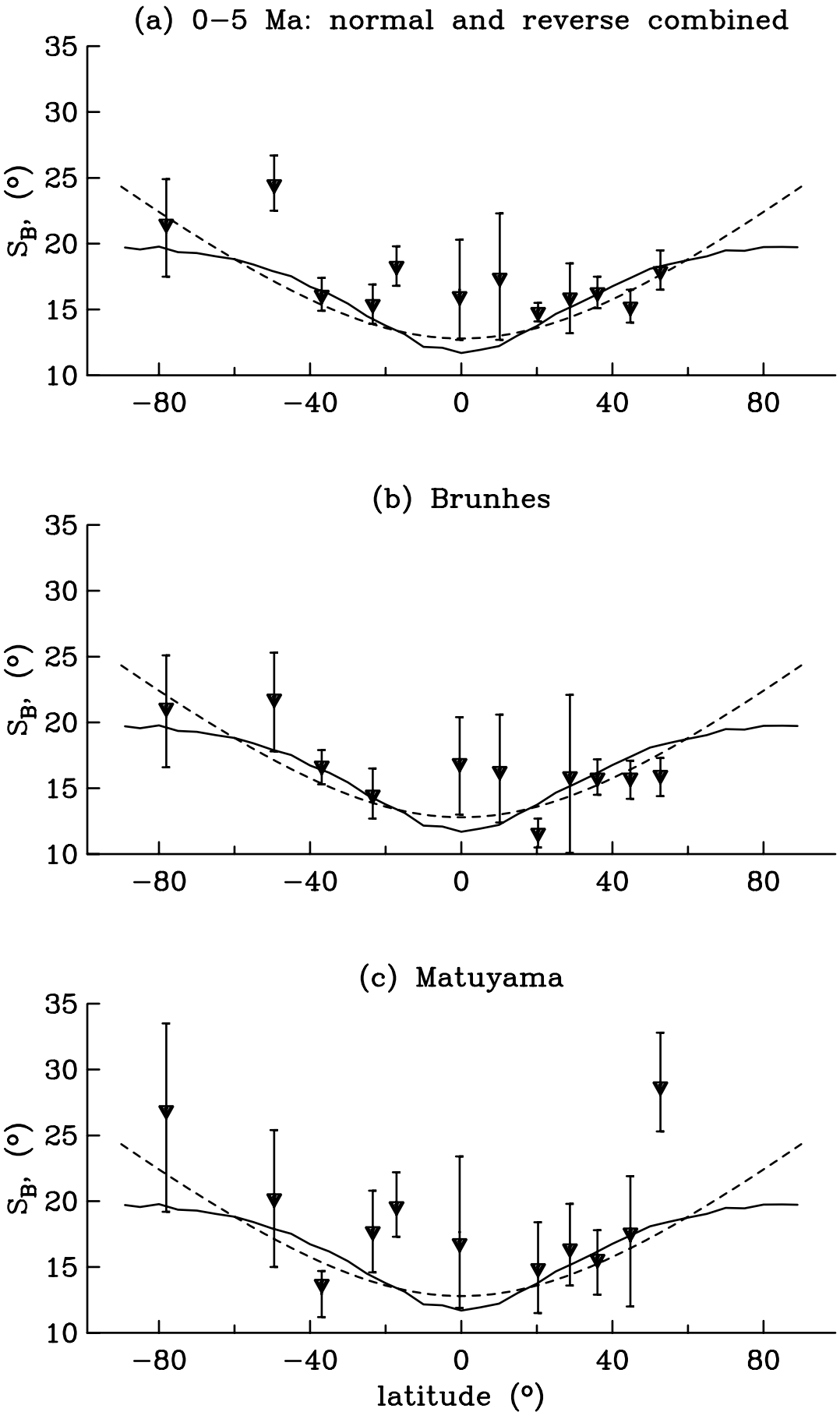
(a) 0–5 Ma: normal and reverse combined
(b) Brunhes
(c) Matuyama
S_B, (°)
35
30
25
20
15
10
−80
−40
0
40
80
latitude (°)

Figure 10